

6. PROTEUS MEASUREMENT TECHNIQUES

For the purposes of this report, the HTR-PROTEUS experimental methodologies have been described under five headings:

1. Critical loadings
2. Reactivity
3. Kinetic parameter
4. Reaction-rates
5. Absorption cross-section of the reactor graphite

These categories do not differentiate between individual measurement techniques as such, but rather between the experimental determination of different parameters, each of which may involve the use of several different individual measurement techniques. Furthermore, the same measurement technique may appear under more than one heading, e.g. the Pulsed Neutron Source measurement technique appears in three of the five categories.

The descriptions which follow include the theoretical basis, the practical application and the analysis strategy of each method. It is not intended to present an exhaustive description of each technique. The interested reader is invited to refer to the large number of technical reference documents for further details of the experiments. In particular, the three doctoral theses of Rosselet, Wallerbos and Köberl [6.1, 6.2, 6.3] present in sufficient detail the experimental techniques used for the reactivity, kinetic parameter and reaction rate measurements. Last, but by no means least, it should be mentioned that, during the course of the programme, a great deal of experimental development work has been carried out, which has to a great extent, solved the problems associated with measurements in such systems. Although the results of techniques developed are presented in chapters 7 and 8 of this work, the details of the experimental developments are well outside the scope of the present document. In depth descriptions however can be found in the various documents referred to in this chapter.

6.1. CRITICAL LOADINGS

The “approach-to-critical” for each configuration was accompanied by the usual *inverse counts versus core loading* plot with an extrapolation to $1/\text{counts} = 0$ being made after each pebble loading step to give the predicted critical loading (see for example reference [6.4]). After the first two loading steps, which were administratively limited to 1/3 and 1/6 of the number of pebbles predicted for the critical loading respectively, the remaining steps were limited [6.5] to one half of the predicted additional number of pebbles required to achieve criticality or the worth of the control rod bank, whichever was the larger. The count rates were measured using neutron detectors situated in the radial reflector. Because the loading of a pebble bed involves a continuous core height and thus core-detector geometry change, it was expected that the approach curves would show considerable spatial dependence and for this reason, early loadings were monitored with additional detectors. The approach curves showed considerable non-linearity for detectors close to the core, with a noticeable effect as the core upper surface reached the axial position of the detector. For this reason, all subsequent approaches were made with detectors situated further out in the radial reflector. A full account of a typical approach is given in [6.4].

Criticality is established and power is raised by means of movements of the control rods. Criticality is maintained by means of the autorod, which is a single, radial-reflector-based rod

driven automatically by the signal from a “deviation channel”, to maintain reactor power and thus criticality. Since the deviation channel comprises an ionization chamber situated in the radial reflector, the signal noise and hence the accuracy of the determination of a critical configuration is determined by the flux level in the reactor. However, the autorod itself has typically a total worth of less than 0.1\$ and the uncertainty in its position represents much less than $\pm 5\%$ of this range, even at relatively low fluxes. Such an uncertainty of $< \pm 0.005\%$ is regarded as negligible.

Although the HTR-PROTEUS system is a reasonably clean one, some correction to the critical state must be made for excess reactivity due to effects such as control rod/autorod insertion at critical, reactor instrumentation in the system etc. To this end, the individual, differential control-rod worths were measured in every configuration and the magnitude of all other effects estimated by means of the compensation technique using these calibrated rods (see for example [6.6]). For reasons of time, these component worths were only measured in selected cores and the values for all other intermediate configurations inferred from the differences between control rod bank worths. These corrections to the actual critical loading to yield the clean-critical loadings are given for each configuration in Section 7.2.

As described in Section 4.2, the various PROTEUS configurations comprised both random and deterministic (hexagonal close-packed and columnar hexagonal) loadings of pebbles, both of which require some careful consideration with regard to the establishment and definition of a critical loading.

6.1.1. Random

Fuel and moderator pebbles, in the desired ratio, were introduced to the cavity in a stepwise manner from a height above the core of about two meters (in order to encourage a truly random arrangement of pebbles). The loading process was carried out automatically with the aid of a pneumatic fueling machine, which was developed specially for the purpose and helped to considerably reduce operator doses during loading and unloading of the various configurations. Since the fuel and moderator pebbles are stored and delivered to the core separately, the first random loading (Core 4.1) was made by simply clamping the fuel and moderator pebble delivery tubes together in parallel and allowing each pebble to fall under gravity into the core from its respective tube. However, it was feared that this may lead to some unwanted ordering effects and indeed a visual inspection during loading suggested some asymmetry (the fuel and moderator pebbles could be differentiated by different surface finishes and by means of a ring inscribed on the fuel pebbles). Consequently, in all subsequent loading operations, the fuel and moderator channels were combined, by means of a simple, funnel-type arrangement, to alleviate this problem.

Having achieved a critical loading, the definitive measured parameter is the number of fuel and moderator pebbles loaded. In the deterministic cores, pebble accounting is simplified by virtue of the fact that it is well known how many fuel and moderator pebbles should reside in each layer and this can be compared, following the loading of each layer, with the number of pebbles registered as having left the fueling machine. In the random cores however this additional check is not possible and, as an additional precaution, having achieved criticality the number of pebbles remaining in the respective storage containers is compared with the expected value.

For random cores, the configuration is not fully defined until the core height and thus the core packing density is also determined. The packing fraction will not necessarily be equal to the theoretical random packing fraction of 0.62 [6.7] due to the presumably significant boundary (ordering) effects in the relatively small cavity. Special core cavity floor inserts were used for the random configurations to reduce such ordering effects. In the particular case of the random configurations, the determination of the core height is not straightforward and introduces a significant uncertainty to the definition of the system state. After a critical state had been achieved, the upper surface of the pebble bed was gently ‘flattened’ to achieve an optically even upper surface without compacting the pebble-bed. The average height of the top of the pebble bed was then determined in several radial directions. It was considered necessary to attribute an uncertainty of some 3cm (half a pebble diameter) to this value. The core heights and associated core packing fractions are summarized in Section 7.2.

6.1.2. Deterministic

The deterministic configurations were loaded by hand. Although the fueling machine was used to deliver pebbles to the loading personnel, each pebble had to be located effectively by hand. In order to facilitate access to the pebble bed, a specially constructed, shielded, “loading-basket” was used. The loading of the hexagonal close packed lattices was relatively simple, since the pebbles located themselves readily in the depressions between the pebbles in the layer below. The loading of the point-on-point cores however, presented more problems; namely in the support of half-finished layers. To this end, special anodized aluminum “tripods” were constructed, which could be removed once the layer was complete. The success of these simple devices represented a major benefit to the project as a whole, since a great deal depended upon the successful and efficient loading of point-on-point cores.

Although the deterministic loadings are significantly more time consuming to load, they possess several distinct advantages compared with the random loadings, including reproducibility and experimental access to the core center. One disadvantage however is that, as a result of the layered nature of these configurations and the fact that the worth of the top layer is often significantly larger than the control rod bank, it is not guaranteed that a satisfactory critical state will be achieved with a complete upper layer of pebbles. In the case of the hexagonal close packed lattice, this represents only a calculational inconvenience and a reduction in the “cleanness” of the calculational model, but in the case of the columnar hexagonal configurations it is somewhat more problematic since it is impossible, in this configuration, to load a partial layer of pebbles. For this reason, it has been necessary in some cores to load mixed final layers consisting of central fuelled regions and outer, pure moderator regions. As a final point it should be noted that, due to the fact that the worth of a pebble varies radially across the core, it is not sufficient in such cases to specify the number of pebbles in a deterministic loading - the precise geometry of the upper layer must also be specified.

6.2. REACTIVITY MEASUREMENTS

As stated in Section 2.4, accurate measurements of the reactivity worth of control absorbers in the core and reflector of configurations with a range of moderation properties was a very important aspect of the HTR-PROTEUS experimental program. Since HTR-PROTEUS was the first series of PROTEUS configurations which were self-critical (as opposed to driven) systems, there was little detailed experience in absolute reactivity measurements. Therefore, during the planning phase of the experiments, an extensive survey of all the commonly used

techniques was made, in order to assess the potential of the various methods and ultimately to decide which ones would be used for the experiments. The criteria on which this decision was made were as follows:

- the method must be compatible with small, highly reflected thermal systems
- the method must be applicable to deeply subcritical cores
- there must be as little dependence upon calculation as possible
- the accuracy of the method should be greater than the current physics methods for LEU HTRs
- the methods chosen should be complimentary techniques, which are, as far as possible, subject to different systematic errors or uncertainties [6.8]
- the economics of the method should be justifiable.

The methods considered comprised subcritical source multiplication, inverse kinetics, reactor noise and pulsed neutron source.

In connection with this preliminary work, IAEA supported visits were made, by a member of the PROTEUS team, both to the VHTRC facility at JAERI to gain “hands-on” experience of pulsed neutron techniques and to KFA Jülich where discussions were undertaken with scientists who had worked on the critical experiments on KAHTER. The conclusions of these discussions are summarized in [6.9]

Ultimately it was decided, on the grounds of applicability, complementarity and required effort, that the Pulsed Neutron Source (PNS) and Inverse Kinetics (IK) techniques would be the main “in-house” reactivity measurement techniques applied to HTR-PROTEUS. Furthermore, it was concluded that neutron noise measurements, although of some academic interest, would not be applied; as a result of the known difficulty of application to slow (long prompt generation time) systems and the large anticipated development effort required. In addition, noise measurements were not regarded as being complimentary to the inhour variation of the PNS technique (see later), since both methods are based upon the isolation of the prompt decay constant and the use of a calculated generation time to yield a value of reactivity in dollars (as it happens, a series of noise measurements were made by a visiting guest scientist, the results of this work being found in the thesis of Wallerbos [6.2]). The results of IK analysis, on the other hand, are very insensitive to estimates of the generation time and furthermore IK is regarded as a dynamic technique (e.g. rod drop from an initially critical state) whereas both noise and PNS are static techniques, which can be applied directly to a subcritical configuration without reference to a critical state.

What will be described below is the classical theory of pulsed neutron and inverse kinetic analysis. During the latter part of the HTR PROTEUS experimental programme, the classical methods were developed and applied in new ways to try and avoid the use of large correction factors. These developments, which are described in detail in [6.1], [6.10], [6.11] contributed significantly to improving the accuracy of the reported measurements and these measurements are reported in sections 7 and 8. A description of the new techniques which above all are based upon the use of epithermal detection systems is beyond the scope of the present work

6.2.1. Pulsed Neutron Source Measurements

Preliminary investigations of the applicability of PNS techniques to subcriticality measurements in HTR-PROTEUS were reported in [6.9, 6.12].

6.2.1.1. Theory

The possibility of using pulsed neutron sources to measure subcriticality was first suggested in the 1950's by Sjöstrand [6.13] and by Simmons and King [6.14]. During the 1960's and early 1970's a great deal of work was carried out on improvements to- and applications of these basic techniques [6.15-6.19] but, in principle, all the techniques fall into one of the two categories - *area-ratio* or *inhour*. The theory of each of these two methods and the specific application of each of the techniques to HTR-PROTEUS will now be summarized:

6.2.1.1.1. *Inhour Method*

The theory of this method is described in [6.14, 6.12] and is discussed, in some detail, in [6.20].

The theory is based, as the name suggests, upon the well-known inhour equation, which is a single energy-group, quasi time-dependent representation of a point reactor system (for a derivation see [6.21, 6.20]). The inhour equation can be written as

$$\rho(\$) = \frac{\Lambda\alpha}{\beta_{eff}} + \sum_{i=1}^n \frac{\alpha b_i}{\alpha + \lambda_i} \quad (6.1)$$

in which:

$\rho(\$)$ is the reactivity in units of dollars

Λ is the prompt neutron generation time

n is the number of delayed neutron groups

α are the $n + 1$ solutions, or roots, of the inhour equation ($n = 6$ in this work)

λ_i is the decay constant for the i th delayed neutron group

b_i is the fraction of delayed neutrons in the i th group (normalised such that $\sum_{i=1}^n b_i = 1$)

β_{eff} is the total effective delayed neutron fraction

For a subcritical system, all $n + 1$ values of α are negative and one, the most negative, is known as the *prompt decay constant* (α_0). The prompt decay constant depends strongly upon the reactivity of the system whereas the other n values are bounded by the decay constants of the delayed neutron precursors and depend only weakly upon reactivity. The basis of the inhour analysis of PNS measurements is to isolate the single exponential α_0 from the delayed background and to use this, with a knowledge of $\lambda_i, b_i, \beta_{eff}$ and Λ , to derive a value of the reactivity in dollars via equation (6.1). One of the main advantages of this technique is that the α s are global parameters of the system and do not depend greatly on experimental conditions, such as detector position.

In systems with relatively short generation times (e.g. light water reactors) $|\alpha_0|$ is found to be $\gg |\lambda_i|$ and the following approximation is true:

$$\rho(\$) \cong \frac{\Lambda\alpha}{\beta_{eff}} + 1 \quad (6.2)$$

In slow, graphite moderated systems such as HTR-PROTEUS however, α_0 is similar in magnitude to the most negative value of λ_i , (-3.87 for ^{235}U) especially when close to critical,

and the approximation in (6.2) is not valid (this corresponds to a situation in which the prompt decay in Figure 6.5 merges into the delayed background). It is still true to say, however, that the dependence of the derived value of $\rho(\$)$ on the second term in equation (6.1) is a second order one and that the most important parameter required to convert α_0 into $\rho(\$)$ is the reduced generation time Λ^* ($\equiv \Lambda / \beta_{eff}$). Now, early studies [6.9] assumed the invariance of Λ^* with $\rho(\$)$ such that:

$$\rho(\$) = \frac{\alpha - \alpha_c}{\alpha} \quad (6.3)$$

in which α_c is the value of α at critical (the subscript 0 has now been dropped but unless otherwise stated is implied)

However, for most applications of the technique, it is unacceptable to assume the invariability of Λ^* . On the other hand, if a value of Λ^* , calculated for the subcritical state of interest is used in equation (6.1), then a direct dependence of the measured result upon calculation is obtained and this is also undesirable. The Japanese tried to avoid this dependence in the following manner [6.22]:

Using the fact that

$$\Lambda_c^* \alpha_c + \sum_{i=1}^n \frac{\alpha_c b_{ic}}{\alpha_c + \lambda_i} = 0 \quad (6.4)$$

and combining equations (6.1) and (6.4), we obtain:

$$\rho(\$) = \left(\frac{\alpha - \alpha_c}{\alpha_c} \right) \cdot f + \varepsilon_1 + \varepsilon_2 \quad (6.5)$$

in which

$$f = \alpha_c \sum_{i=1}^n \frac{b_{ic}}{\alpha_c + \lambda_i} \quad (6.6)$$

$$\varepsilon_1 = \alpha (\Lambda^* - \Lambda_c^*) \quad (6.7)$$

and

$$\varepsilon_2 = \alpha \sum_{i=1}^n \frac{b_i}{\alpha + \lambda_i} - \alpha_c \sum_{i=1}^n \frac{b_{ic}}{\alpha_c + \lambda_i} \quad (6.8)$$

In this way, the dependence upon Λ^* is reduced to a dependence upon $\Delta \Lambda^*$, the value of which is expected to be less sensitive to the calculational approach chosen. However, it will now be demonstrated that great care must also be taken in the use of this approach: Λ is generally defined [6.23] as *the average time between successive generations of neutrons*, which is equivalent to the inverse neutron production rate and can be written mathematically, in the formulation of first-order perturbation theory, as:

$$\Lambda \equiv \frac{1}{F} \iint \phi_{c,static}^+(r, v) \frac{1}{v} \phi_{c,static}(r, v) dr dv \quad (6.9)$$

in which

$\phi_{c,static}(r, v)$ is the forward, static, neutron flux at critical

$\phi_{c,static}^+(r, v)$ is the adjoint of the static, neutron flux at critical

$\frac{1}{v}$ is the inverse velocity in seconds

F is an arbitrary normalisation factor [6.20]

However, this formulation, incorporating as it does only critical flux shapes, makes no sense in the present context since it implies a value of Λ which is invariant with flux, and hence reactivity, changes. A more reasonable approach would be to use the perturbed fluxes $\phi_p^+(r, v)$ and $\phi_p(r, v)$ and a further improvement would be to use a *kinetic* flux distribution as the forward flux. This approach was suggested by Difilippo [6.24] in which Λ was defined as follows

$$\Lambda \equiv \frac{1}{F'} \iint \phi_{p,static}^+(r, v) \frac{1}{v} \phi_{p,kinetic}(r, v) dr dv \quad (6.10)$$

For the sake of consistency, it is also possible to define the effective delayed neutron fraction in this manner, although it was demonstrated in [6.20] that the effect is much less significant:

$$\bar{\beta}_i \equiv \frac{1}{F'} \iiint \tilde{\chi}_i(v) \beta_i v \Sigma_f(r', v') \phi_{p,static}^+(r, v) \phi_{p,kinetic}(r, v) dr dv dr' dv' \quad (6.11)$$

in which:

$\tilde{\chi}_i$ is the normalised fission spectrum of delayed group i

v is the average total number of neutrons produced per fission

A physical justification for the use of kinetic and not static fluxes comes from the fact that the PNS measurement is made in a decaying system in which kinetic fluxes predominate.

A thorough quantification of the differences in $\Delta\Lambda$ and β_{eff} resulting from these various definitions is presented in [6.20] and here it is seen that, in particular, unless equation (6.10) is adopted, significant errors can occur in the estimate of reactivity. This approach was therefore adopted in the analysis of all PNS, inhour-type measurements described in this report.

6.2.1.1.2. Area-ratio Method

The original applications of the Area-ratio method [6.13] were made on water-moderated systems in which it can be assumed that $\alpha_0 \gg \lambda_i$. Under this assumption, it is possible to write that:

$$\rho(\$) = \frac{\int \phi_{prompt} dt}{\int \phi_{delayed} dt} = \frac{\text{prompt area } (A_p)}{\text{delayed area } (A_d)} \quad (6.12)$$

Again, this assumption is not valid in an HTR-PROTEUS type system and in this case it can be shown that [6.25]:

$$\rho(\$) = \frac{A_p}{A_d} \sum_{i=1}^n \frac{b_i}{\left(1 + \frac{\lambda_i}{\alpha}\right)^2} \quad (6.13)$$

However, this formulation still suffers from two very serious problems related to the spatial dependence of the results of the analysis. These are:

1. Harmonic distortion
2. Kinetic distortion

These two effects and their correction will now be described:

Harmonic distortion

The excitation of a multiplying system by an external source (or indeed by a rapid change of state like a rod-drop) will inevitably generate short-lived flux modes which are not characteristic of the fundamental (persisting) mode of the system. On time scales of minutes, these harmonics are generally negligible, however, in PNS type measurements in which time scales of the order of milliseconds are observed, such harmonic effects can be significant. Similar, but generally smaller effects are also associated with the delayed neutrons. The latter effect will not be discussed here but is treated adequately in [6.24], as is the calculational correction of the prompt harmonic effects. In this work however, a modification of the method by Sjöstrand, proposed by Gozani [6.15] and known as the *Extrapolated Area-Ratio Technique* or *Gozani method*, is used. In this method, a fit to the linear part of the prompt decay curve is extrapolated back to $t = 0$ to yield a prompt area which is free from harmonic interference.

Kinetic distortion

This phenomenon represents a further departure from point kinetic theory. In the words of Gozani [6.26] the phenomenon can be described as follows: "*Thermal prompt neutrons [in a subcritical system] leaving the core and entering the reflector will return after diffusing for a few generation times. During this time, most of the prompt neutrons belonging to the same generation, initially present in the core, have died away. Thus, there results an accumulation of prompt neutrons in the reflector. The delayed precursors, decaying very slowly, hardly change during the time a thermal delayed neutron diffuses in the reflector. Hence their distribution is very similar to that of the fictitious static, critical system.*"

The phenomenon manifests itself as follows:, Very generally, regions of high absorption in the system tend to have a higher relative delayed background than those in low absorption regions. It is clear that this phenomenon will cause a spatial dependence of the reactivity as defined by equations (6.12) and (6.13) and, since the magnitude of the effect in systems with low absorption reflectors can amount to many tens of percent [6.9, 6.12, 6.24], it must be accounted for. Techniques for its correction are widely available [6.23, 6.18] and were re-worked with the HTR-PROTEUS measurements in mind [6.24]. Although the VHTRC strategy seems to discard the use of calculational corrections in favor of averaging a large number (up to 48) individual responses [6.9], it was considered preferable, in the present work, to adopt an approach involving fewer measurements, each corrected with a calculated factor.

The basis of the original method used to correct for kinetic distortion in HTR-PROTEUS will now be described:

In [6.24] the true reactivity $\rho(\$)$ is shown to be related to the Gozani reactivity $\rho_{GO}(\$)$ in the following manner

$$\rho(\$) = \rho_{GO}(\$)K_d H_d \quad (6.14)$$

in which:

K_d represents the kinetic distortion and

H_d represents the effects of delayed harmonics

Reference [6.24] provides the following definition:

$$K_d(\mathbf{r}) = \frac{N_{p,static}^0(\mathbf{r}) \cdot \langle \phi_{p,static}^{0+} | \chi_s P \phi_{p,kinetic}^0 \rangle}{N_{p,kinetic}^0(\mathbf{r}) \cdot \langle \phi_{p,static}^{0+} | \chi_s P \phi_{p,static}^0 \rangle} \quad (6.15)$$

where

$N_{p,static}^0 = \int \Sigma_d(v) \cdot \phi_{p,static}^0 dE$ - the integrated response of the detector to the perturbed, fundamental mode, static flux

$N_{p,kinetic}^0 = \int \Sigma_d(v) \cdot \phi_{p,kinetic}^0 dE$ - the integrated response of the detector to the perturbed, fundamental mode, kinetic flux

$\Sigma_d(v)$ is the energy dependent detector response

and where the terms in brackets represent normalization factors based upon the total fission neutron production in the kinetic and static distributions respectively. In this case the '0' superscripts indicate fundamental mode values.

As mentioned above, the effects of delayed harmonics are generally small compared with those of kinetic distortion, but for completeness their correction will be defined here:

H_d , the delayed harmonic correction, is defined as:

$$H_d(\mathbf{r}) = \frac{\sum_{n=0}^{\infty} b_n N_{p,static}^n(\mathbf{r}) \cdot \langle \phi_{static}^{0+} | \chi_s P \phi_{static}^0 \rangle}{N_{p,static}^0(\mathbf{r}) \cdot \langle \phi_{static}^{0+} | \chi_s P \phi_{static}^{\Sigma} \rangle} \quad (6.16)$$

In which the summation term indicates a sum over all modes.

As mentioned briefly above, during the course of the programme, novel measurement techniques were developed, in particular involving the use of "epithermal detectors" in place of the usual thermal ones. These developments, described in detail in [6.1] and [6.10] contributed to the significant reduction of the importance of the correction factors described above. Measurements of the new type are reported in Chapters 7 and 8.

6.2.1.2. Experimental Methods

The experimental set-up for the PNS measurements is shown in Figure 6.1. The PNS itself, a miniature accelerator tube (type MF Physics A-801¹) producing 3μs long pulses of 14Mev neutrons via the D-T reaction, was invariably situated in the radial center of the lower axial reflector such that a target (source) - core distance of ~ 70cm was obtained, including some 53cm of graphite (see Figure 6.2). The "pulse unit" also shown in Figure 6.2 was used to simultaneously trigger the PNS and the multi-channel scaler (MCS) system. In order to achieve satisfactory measurement statistics, a large number of responses must be

¹ MF Physics Corporation, 5074 List Drive, Colorado Springs CO 80919, USA

superimposed (typically 500 close to critical and up to 3000 at ~15 \$ subcritical) and it is very important that the pulse and measurement sweeps be well synchronized. In principle it was possible, using the pulse unit, to delay the measurement sweep to account for the finite delay between triggering and neutron production in the PNS, but since this delay is normally of the order of 20 μ sec (compared with a typical MCS channel width of some 1000 μ sec) the effect is negligible.

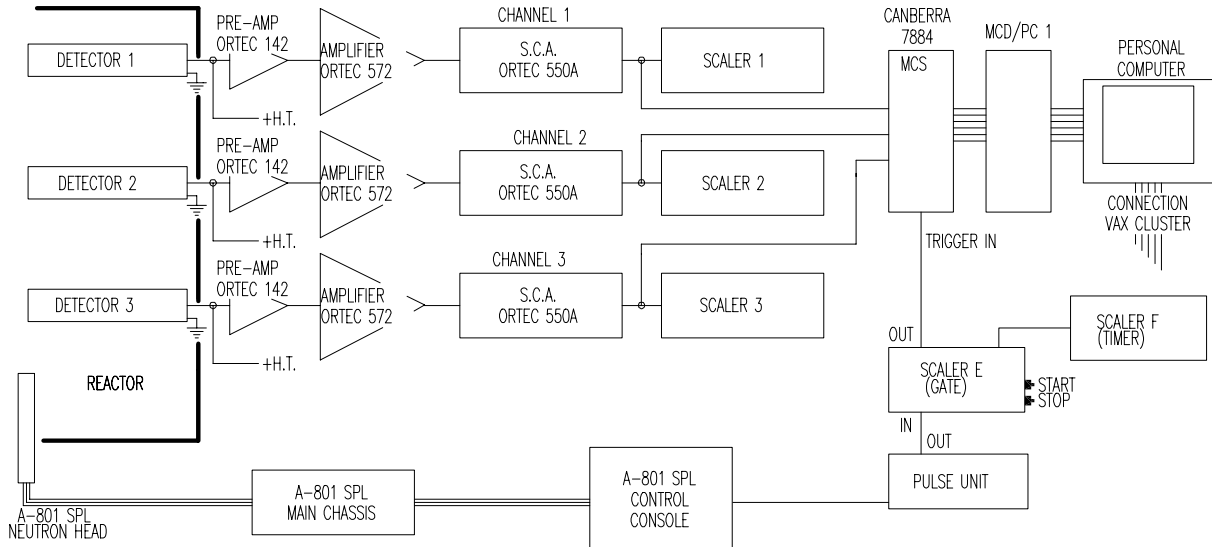


Figure 6.1 A Schematic of the Experimental Set-up Used for PNS Measurements

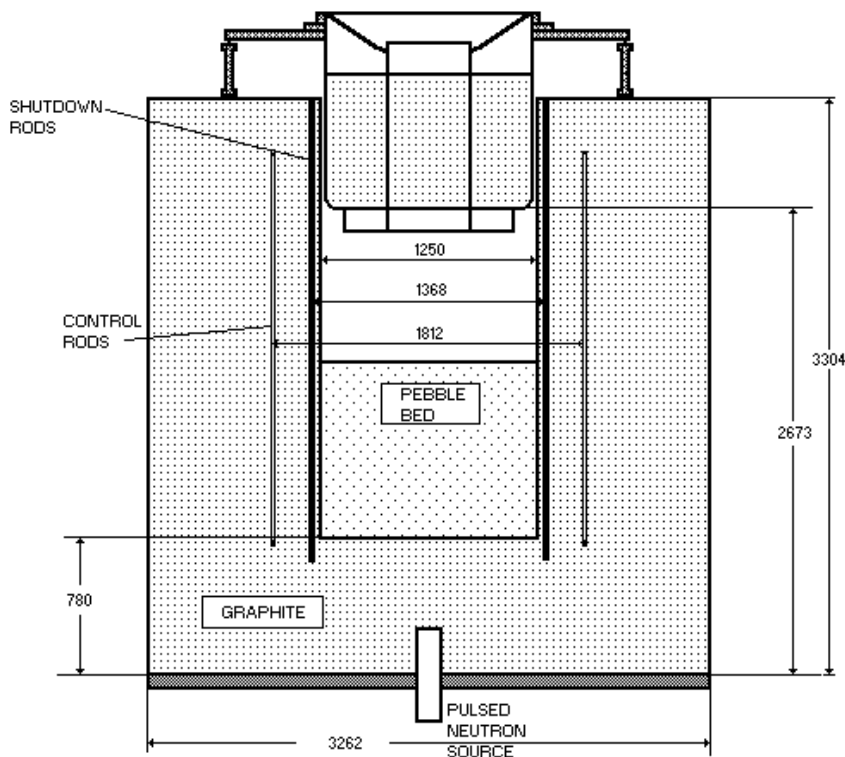


Figure 6.2 Cross-sectional View of the HTR-PROTEUS System Showing the Position of the PNS Unit

Although the PNS unit can operate at a nominal maximum pulsing rate of some 10 pulses per second (PPS) the maximum pulse rate during a particular measurement is determined by the magnitude of the prompt decay constant being measured. A satisfactory analysis of the response can be made when the prompt decay occupies around one half of the sweep time and the pulse rate is adjusted accordingly until as little “dead time” as possible exists between the end of the MCS sweep and the next pulse. This is very important for the area-ratio evaluation in which this dead time must be taken into account in the evaluation of the delayed area (A_d). The following “rule-of-thumb” was normally used to determine approximate values for the pulse-rate (PPS), MCS channel width (CW) and number of measurement channels (NCH) for each configuration:

$$CW(\text{seconds}) \cong \frac{-9.21}{\alpha \cdot NCH} \quad (6.17)$$

$$PPS = \frac{1}{NCH \cdot CW} \quad (6.18)$$

The responses were normally measured with up to three, high-efficiency (0.3 counts per second per unit flux), BF_3 detectors located in various positions around the system. In the epithermal measurements, the detectors were covered in cadmium or indium. Detector positions were chosen to give responses with a range of predicted correction factors but also so as to minimize source harmonic and detection dead-time effects and to optimize counting statistics. The detector sizes were chosen so as to fit into the channels between the pebbles of the deterministic loadings such that measurements in the core itself could be made.

For each measurement of a particular subcritical state, the following procedure, defined in the corresponding measurement plan of the HTR-PROTEUS QA Document (see Appendix) was followed (it is assumed in the following that the measurement system has been properly adjusted and calibrated with respect to detector operating voltages, discriminator settings, detector dead times etc.):

1. The detection system is switched on and allowed to stabilize
2. A critical balance is established with the PNS and neutron detectors in place and the reactor start-up sources withdrawn (to avoid necessary background interference)
3. The autorod (and control rod) positions are frozen
4. The subcritical state of interest is established, this may involve the insertion of the shutdown rods, the removal of the upper reflector, the insertion of a dummy control rod etc.
5. The PNS is switched on and CW, PPS and NCH (invariably 512) adjusted as required. The system is pulsed for ~ 15 minutes, without measuring, to allow an equilibrium state of the delayed neutron background to develop.
6. When a stable equilibrium has been achieved, the MCS is triggered and data is accumulated until satisfactory statistics are obtained.
7. The accumulation is stopped, the PNS is switched off, the total number of measured pulses and the total measurement time are recorded. The raw data is stored on the PC.

8. After a suitable delay, to allow the flux to stabilize, the measurement is repeated, without pulsing, to establish the background contribution to the measurement. Data is stored on PC

6.2.1.3. Data Processing

The measured responses are processed by the FORTRAN code ALPHUBEL.FOR [6.25,6.27,6.28], installed on the PROTEUS VAX 3000/4000 Cluster and written with the experimental needs of PROTEUS in mind. The code carries out the following tasks:

1. Reads in raw data from one detector, subtracts the average background and corrects the contents of each channel for dead time (the dead time of each detection channel was measured on several occasions to be $1.4 \pm 0.1 \mu\text{sec}$)
2. Using input values of β_{eff} , b_i and Λ , calculated in the manner defined in equations (6.10) and (6.11) and an input guess of reactivity (or a value derived from the measurement itself), the inhour equation is solved for its 7 roots (6 group delayed data was invariably used). Using these roots, a simulated PNS equilibrium response is generated and the delayed part is fitted to the delayed part of the measured response (i.e. the second half of the measured response). This approach is necessary in order to predict the delayed response in the first part of the measured distribution (“underneath” the prompt decay). The predicted delayed distribution is then subtracted from the total response, leaving in principle, only measured, prompt neutrons.
3. To this prompt response is then fitted a single exponent, over a range of different start- and end-channels and the value of α corresponding to the fit with the lowest uncertainty is taken and used, along with the input values of β_{eff} , b_i and Λ to derive a “measured value” of reactivity from equation (6.1)
4. The code then returns to step 2 and repeats steps 2 and 3 until a convergence in reactivity is obtained.
5. With the prompt distribution associated with this converged value of reactivity, the following parameters are evaluated:
 - a. A_p and A_d and from this the corrected and uncorrected Sjöstrand reactivity via equations (6.12) and (6.13)
 - b. Using a range of starting and ending channels for the fit to the prompt distribution, a so-called *tornado matrix* is constructed. This technique derives from the analysis of PNS measurements on the Fort St. Vrain Reactor [6.19] and serves to select a fit range which is devoid of prompt harmonics, whilst maximizing the size of the fit range.
 - c. For each position in this matrix, the values of α , ρ_{INH} (equation (6.1)), $A_p^{\text{extrapolated}}$ and $\rho_{\text{GO}}(\$)$ are derived along with their respective uncertainties.

It should be pointed out that the calculated value of generation time must be based on an initial guess of reactivity, which may not be correct. A further external iteration process is then necessary.

The ALPHUBEL.FOR code has been extensively verified and validated by means of the novel use of simulated experiments [6.29-6.31]. Early discrepancies observed between ALPHUBEL and the Japanese analysis route [6.25] were shown not to be due to inadequacies in ALPHUBEL.

Having obtained the tornado-plot for each detector in a single measurement, a single fit position is chosen (by eye) where all detector responses converge within the experimental uncertainty value and hence where prompt harmonics are insignificant. At this position is taken the final value of ρ_{INH} and the final, uncorrected version of $\rho_{GO}(\$)$. Finally, $\rho_{GO}(\$)$ is corrected according to equation (6.14)

6.2.1.4. Uncertainties

Uncertainties normally comprise statistical uncertainties in the measured data, and systematic uncertainties associated with the data used to convert the measured parameter to reactivity.

Statistical uncertainties can be reduced by increasing count rates and measuring times in individual measurements or by repeating measurements. The former method is limited by the particular properties of the counting system, namely dead-time and detector efficiency, and the latter method although effective, is expensive in time and effort.

Reductions in uncertainties associated with the use of a particular set of delayed neutron data in the processing of the measured parameters to yield the desired parameter, in this case reactivity, can only be achieved by using a better data set. This possibility is discussed briefly below.

Although the HTR-PROTEUS system contains two fissionable isotopes, the influence of the ^{238}U represents only a few percent of the total fission yield and has a correspondingly small influence on the delayed neutron properties of the system. Therefore, although the effective delayed neutron yields were calculated properly, taking into account the presence of the ^{238}U , using the perturbation theory code PERT-V, the uncertainties associated with these fractions, and the decay constants and their associated uncertainties were taken directly from the ^{235}U isotopic data. To demonstrate the significance of this approximation, the effective and ^{235}U isotopic group fractions are compared in the Table 6.1 below for the JEF 1 data.

i	²³⁵ U		SYSTEM
	λ_i	b_i	$b_{\text{eff},i}$
1	0.0127±0.0003	0.038±0.004	0.0385
2	0.0317±0.0012	0.213±0.007	0.212
3	0.115±0.004	0.188±0.024	0.188
4	0.311±0.012	0.407±0.010	0.407
5	1.4±0.12	0.128±0.012	0.128
6	3.87±0.55	0.026±0.004	0.026
β_{tot}		0.0071876	0.0072126

Table 6.1: Effect of ²³⁸U on Effective Delayed Neutron Fractions

The value of reduced generation time used in the analysis, was calculated using PERT-V but normalized to a value of Λ/β determined experimentally in each core. For demonstration purposes an uncertainty of 5% was attributed to this parameter here, although this is almost certainly an overestimate and can be reduced in the analyses proper.

		NOMINAL REACTIVITY (\$)			
TECHNIQUE	COMPONENT	-0.15	-1.0	-5.6	-12.0
<i>Inhour</i>	α	-4.88±0.75%	-7.79±0.4%	-27.9±0.4%	-55.3±0.3%
	$\alpha\Lambda^*$	-1.33±5.0%	-2.09±5.0%	-6.54±5.0%	-12.5±5.0%
		(±0.75%)	(±0.4%)	(±0.4%)	(±0.3%)
	$\sum_{i=1}^6 \frac{\alpha b_i}{\alpha + \lambda_i}$	-1.19±6.6%	-1.07±3.1%	-1.02±3.0%	-1.01±3.0%
		(±0.4%)	(±0.2%)	(±0.2%)	(±0.14%)
	Total ρ	-0.15±68%	-1.01±11%	-5.52±6%	-11.5±5.5%
		(±7.5%)	(±0.8%)	(±0.5%)	(±0.3%)
<i>Sjöstrand</i>	delayed area	3.2E7±0.02%	3.4E6±0.05%	1.3E5±0.3%	7.8E4±0.36%
	prompt area	2.8E6±1.0%	2.9E6±0.1%	7.5E5±0.14%	9.1E5±0.13%
	prompt/delayed	0.087±1.0%	0.835±0.13%	5.684±0.3%	11.58±0.37%
	$\sum_{i=1}^6 \frac{b_i}{\left[1 + \frac{\lambda_i}{\alpha}\right]^2}$	1.779±27%	1.182±3.6%	1.034±3.0%	1.016±3.0%
	Total ρ	-0.156±27%	-0.987±3.6%	-5.879±3.6%	-11.77±3.0%
<i>Gozani</i>	intercept	2.2E4±1.4%	3.4E4±0.9%	1.7E4±1.2%	2.0E4±0.8%
	α	-4.88±0.75%	-7.79±0.4%	-27.9±0.4%	-55.3±0.3%
	delayed area	3.2E7±0.02%	3.4E6±0.05%	1.3E5±0.3%	7.8E4±0.36%
	uncorrected ρ	0.091±1.6%	0.854±1.0%	5.65±01.3%	11.4±0.9%
	$\sum_{i=1}^6 \frac{b_i}{\left[1 + \frac{\lambda_i}{\alpha}\right]^2}$	1.779±27%	1.182±3.6%	1.034±3.0%	1.016±3.0%
	Total ρ	-0.163±27%	-1.01±3.7%	-5.84±3.3%	-11.59±3.1%

Table 6.2: Typical Uncertainties for the Three PNS Techniques, Over a Range of Reactivities.

Table 6.2 summarizes typical uncertainties for the three PNS techniques, over a range of reactivities.

The following points are worthy of note:

- at subcriticalities of less than $\sim 1\%$, the uncertainties on all three techniques are unacceptably large. In the case of the inhour technique, this is because the prompt and delayed terms in the inhour equation are very similar, leading to a small value with a large uncertainty. In the case of the area ratio methods, the cause is the large value of the uncertainty on the correction factor $\sum_{i=1}^6 \frac{b_i}{\left[1 + \frac{\lambda_i}{\alpha}\right]^2}$
- at deeper subcriticalities, the uncertainties rapidly decrease. In the inhour method, the uncertainty tends to that on the generation time as we approach the prompt approximation. For the area ratio methods the limit is the 3% error on the correction factor.
- the statistical uncertainties in all three methods are seen to be insignificant compared with those associated with the delayed neutron data.

6.2.2. Inverse-kinetics

The Inverse Kinetics (IK) technique was chosen on the grounds that it is complementary to the PNS method, and that it is relatively easy to implement, with no special equipment or expertise required.

The basic principle of the method is that $n(t)$, the evolution of the neutron density following a reactivity perturbation to a critical system at time $t = 0$, can be related to the size of the reactivity perturbation. This perturbation can take any form, slow or fast, positive or negative, although the most common case is a “control-rod drop” in which one or more absorber rods fall into the system under gravity. A complete IK analysis would require three-dimensional, time-dependent theory in which all transient harmonic and spatial effects were modeled. Although considerable attention has been paid in the literature to transient harmonic effects during rod-drops, e.g. [6.32], the effect is not considered to be important for the current measurements, especially as the aim of the measurements is generally to obtain integral rod worths and not details during the rod drop itself [6.33]. It was therefore considered to be a very good first order approximation, to concentrate on spatial effects alone.

Because of the inherent difficulties in solving the time-dependent neutron transport equation in its general form, IK analysis is normally limited to a single-energy group, point reactor representation with 6 delayed neutron groups. However, the dropping of an absorber into the system not only causes a reduction in reactivity and a consequent decay in the space-integrated neutron density, but also a disturbance in the local neutron density distribution and its energy distribution. Any neutron detector placed within or close to the system will therefore experience both global and local effects. In short, a method must be available to convert space and detector dependent measurements to a global value of reactivity. In principle it would be possible to make many measurements around the system and to average the results in some way. However the large experimental effort required and the question of how to weight the individual measurements calls for a more sophisticated approach. One such approach is described in detail in [6.33], and is that which is adopted in this work.

6.2.2.1. Theory

The basic point reactor theory of this technique has been exhaustively described elsewhere (see for instance [6.33-6.35]) and will only be briefly summarized here. The theory and techniques for the correction of the results to account for departures from the point-reactor model will be dealt with in somewhat more detail.

Although it has already been said that the general IK theory can be applied to both negative and positive reactivity perturbations, the HTR-PROTEUS approach treats the two cases in a slightly different way.

6.2.2.1.1. Negative Reactivities

The starting point is the point kinetics equations with six delayed-neutron groups:

$$\frac{dn(t)}{dt} = \frac{\rho(t) - 1}{\Lambda^*(t)} \cdot n(t) + \sum_{i=1}^6 \lambda_i c_i(t) + S \quad (6.19)$$

$$\frac{dc_i(t)}{dt} = \frac{b_i}{\Lambda^*(t)} \cdot n(t) - \lambda_i c_i(t) \quad (6.20)$$

in which

$n(t)$ represents the time dependent neutron density in the fictitious point reactor.

(The relationship of this parameter to $q(t)$, the response measured in a real reactor, will be defined later)

c_i is the concentration of delayed neutron precursors in group i

Re-arranging equation (6.19), integrating equation (6.20), with the boundary condition that at $t=0$, $\rho=0$, $n(t)=n(0)$ and $c_i(t)=c_i(0)$ and combining the two equations yields:

$$\rho(t) = 1 + \frac{1}{n(t)} \left[\Lambda^*(t) \frac{dn(t)}{dt} - n(0) \sum_{i=1}^6 b_i e^{-\lambda_i t} - \sum_{i=1}^6 b_i \lambda_i \int_0^t e^{-\lambda_i (t-t')} n(t') dt' \right] \quad (6.21)$$

in which, the external source term S has been ignored and in which it will be noted that, since the factor $n(t)$ appears in the numerator and denominator of each term in the square brackets, its normalization is arbitrary and we could write the equation in terms of $N(t)$ where $N(t) = n(t)/n(0)$

It is seen from equation (6.21) that, with a knowledge of the initial flux level, the variation of this flux with time and calculated values of b_i and Λ^* , the reactivity (in dollars) as a function of time can be derived. This equation is the basis of the so-called *differential method* and corresponds to the most general expression of inverse kinetics. It can be applied to both negative and positive reactivities, but has been applied mainly to the former in HTR-PROTEUS. It should be noted that, under all practical circumstances, the first term inside the square brackets is negligible, with the consequence that, in contrast to the PNS techniques, this method has a negligible dependence upon the generation time. Furthermore, although it is true to say that this method can be used to provide a truly time-dependent reactivity, and thus that the speed of the reactivity change is immaterial, it is nevertheless preferable, in the cases where only an integral worth is required to ensure that the perturbation occurs as quickly as

possible such that the flux level is still high enough to provide satisfactory counting statistics when the perturbation is complete.

A simplification of this method, due to Hogan [6.36], applies the operator $\int_0^\infty dt$ to equations (6.19) and (6.20) before combining. The following relationship is obtained:

$$\rho = \frac{\Lambda^* + \sum_{i=1}^6 \frac{b_i}{\lambda_i}}{\int_0^\infty n(t) dt} \quad (6.22)$$

Equation (6.22) is only valid for an instantaneous reactivity change. For reactivity changes taking place over times comparable to the time constants of the system, a correction must be made to equation (6.22) such that:

$$\rho = \frac{\Lambda^* + \sum_{i=1}^6 \frac{b_i}{\lambda_i}}{\int_0^\infty n(t) dt - \int_0^{t_D} [1 - f(t)] n(t) dt} \quad (6.23)$$

In which $f(t)$ (with boundary conditions $f(0) = 0$, $f(t \geq t_D) = 1$) corrects the equation for the time required to make the reactivity step. This method is known as the *integral* method and it is clearly more important in this case to ensure that perturbation occurs as rapidly as possible. Again, the generation time term appearing in the numerator is, in most practical cases negligible.

It is not possible, in practice, to measure directly the neutron densities $n(t)$ referred to in equations (6.19)-(6.23), since these are *global* parameters and we are restricted to *local* measurements. It is only possible to measure $q(r, t)$, the response to a flux $\phi(r, v, t)$ using a detector having cross-section $\Sigma_d(v)$

i.e.

$$q(t) = \langle \Sigma_d(v) \phi(r, v, t) \rangle \quad (6.24)$$

where the brackets indicate integration over energy and over the detector volume

Now, assuming that the local $\psi(r, v, t)$ and global $h(t)$ changes in neutron population are separable, we can write:

$$\phi(r, v, t) = \psi(r, v, t) h(t) \quad (6.25)$$

in which $\psi(r, v, t)$ represents the spatially dependent change in neutron population; for example the perturbation caused by a dropped absorber rod, and is only time dependent insofar as the population changes during the rod drop but is static before and after the rod drop (in the absence of harmonic effects). On the other hand $h(t)$ represents the global change in system flux and is time dependent as a result of the decay of the prompt and delayed neutron populations following the rod drop. Therefore, combining (6.24) and (6.25):

$$q(t) = \langle \Sigma_d(v) \psi(r, v, t) \rangle h(t) \quad (6.26)$$

or, relative to the response at critical ($h(0)=1$):

$$Q(t) \equiv \frac{q(t)}{q(0)} = \frac{\langle \Sigma_d \psi(r, v, t) \rangle}{\langle \Sigma_d \psi(r, v, 0) \rangle} h(t) \quad (6.27)$$

more explanation in refs [6.28, 6.32]

and thus

$$N(t) = \frac{n(t)}{n(0)} = Q(t) \left[\frac{\langle \Sigma_d \psi(0) \rangle \Lambda(t) P(t)}{\langle \Sigma_d \psi(t) \rangle \Lambda(0) P(0)} \right] \quad (6.28)$$

in which

$P(t) \equiv \langle \chi_s P \psi(t) \rangle$ the total fission neutron production at time t

The term in brackets in equation (6.28) is the calculated correction factor with which we correct the normalized measured response $Q(t)$ to the value required in equations (6.21) and (6.23); namely $N(t)$ (see also [6.38]).

As mentioned above, during the course of the programme, novel techniques were developed to reduce the effects of distortions requiring calculated factors. Thus, “epithermal IVK” was developed, whose theory is beyond the scope of the present document, but which is adequately described in [6.1] and [6.10]

6.2.2.1.2. Positive Reactivities

The previous techniques are useful for the measurement of reactivities in the approximate range $+0.1\% \rightarrow -15\%$. For small positive reactivities it is also possible, and somewhat more convenient, to utilize the well known *stable period* technique. This technique was exclusively used for the differential calibration of control-rods in HTR-PROTEUS (see for example [6.39, 6.40]) and its theory will now be briefly summarized:

The solution of the inhour equation, with six delayed neutron groups, for a positive reactivity step, yields 7 roots, 6 of which, $\alpha_0, \dots, \alpha_5$, are negative and one of which, α_6 is positive. α_6 is known as the persisting root and is that which ultimately determines the positive period of the system. In short, the asymptotic time dependence of the supercritical reactor is determined by

$$n(t) = A e^{\alpha_6 t} \quad (6.29)$$

Therefore, by fitting the measured asymptotic flux increase to a curve of the form of equation (6.29), a measured value of α_6 is obtained which can be fed into equation (6.1) along with calculated values of Λ^* , β_i and λ_i to give a value of reactivity (in dollars) for the step change.

One advantage of this technique is that the α_i are global values of the system and thus no spatial dependence of the measurements is observed. Furthermore, in common with the method described in Section 6.2.2.1.1., the results are very insensitive to the value of Λ^* used. On the other hand, there is a heavy reliance upon the delayed neutron constants, a fact which is shown to have possible serious implications with respect to the use of the ENDF/B-VI data .

The implementation and testing of this technique for HTR-PROTEUS is described in [6.41]

6.2.2.2. Experimental Methods

The experimental set-up for positive reactivities was very similar to that used for the PNS technique, except that in place of the high efficiency detectors, low efficiency ones ($\sim 10^{-3}$ counts per second per unit flux) were used, in order to permit measurements at the normal PROTEUS operating fluxes of $10^7 - 10^9 \text{ n.cm}^{-2}.\text{s}^{-1}$. For the negative reactivities (rod-drops) two different set-ups have been used:

6.2.2.2.1. Negative Reactivities

The most important requirement for a measurement system for use in rod-drop measurements is a small detection dead time. This arises from the fact that, in the name of good statistics it is desirable to have as high a count rate as possible at critical, before the rod-drop, so that the statistics after the rod-drop are still satisfactory. Two approaches have been taken in the HTR-PROTEUS experiments to fulfil this requirement:

1. Early on in the project, low dead time detectors were not available and the same detectors as were used for the PNS measurements had to be used, these having dead times of some $1.4 \pm 0.1 \mu\text{sec}$. Because it was found that the use of these detectors alone led to unacceptably large uncertainties on the derived reactivities, a method was developed in which two detectors, having different sensitivities, were used, situated close together in the system. Because the detectors were of high efficiency, they could only be placed on the outer surface of the system (for a discussion of the benefits of this choice, see [6.38]). The responses of these two detectors were then fitted over a small overlap range directly following the rod-drop to give a composite response with the effect of a time-dependent sensitivity. Although this approach was somewhat messy and time consuming, it was unavoidable in the early stages of the program and was shown to give reliable results.
2. From Core 5 onwards, a new (to PROTEUS) measuring system became available, which had previously been used for IK measurements on the SAPHIR reactor and had the advantage that it possessed a very small dead time with each amplified pulse having a width of only a few nanoseconds [6.42]. With this system it was possible to approach count rates of some 800000 counts per second without significant dead time effects.

Apart from these differences in experimental set-up, all rod-drop measurements were carried out in a similar manner, namely:

1. Establish a critical state, with the reactor start-up sources withdrawn and the required detectors in place. When stable, freeze all control absorbers.
2. Trigger the MCS system, which has been set up with a channel width of 0.1 seconds and at least 2048 measurement channels. Although some schemes in the past have used a channel width which varies throughout the measurement, i.e. wide channels before, fine channels during and wide channels again after the drop, a simple approach was taken here in which an intermediate width channel was taken throughout the measurement. The value of 0.1s was chosen as a result of extensive investigations involving the use of simulated measurements, which showed that the use of channel widths greater than 0.1s led to systematic errors in the estimation of reactivity, due to

an inability to resolve the “drop-region”. On the other hand, narrower channel widths led to very poor statistics and significant “rounding-down” effects (see Section 7.5)

3. After a nominal 20s, to establish the initial critical flux level and to measure the initial reactivity (nominally 0), the required shutdown rod configuration (normally 1, 2, 3 or 4 rods, occasionally 8) is dropped.
4. The same measurement is repeated to check for reproducibility and to reduce uncertainties
5. The same configuration is measured with the detectors in a different position in the system, to provide measurements of the same parameter with different spatial correction factors

6.2.2.2.2. *Positive Reactivities*

As mentioned above, the experimental set up for the stable period measurements was very similar to that used for the PNS measurements. The experimental procedure was as follows:

1. Establish a critical state with the required detectors in place. When stable, freeze all control absorbers
2. Trigger the MCS system, which has been configured with a channel width of 1 second and 4096 measurement channels.
3. After a nominal 20s (to establish a start reactivity, nominally = 0.0, but cannot be judged exactly due to drift, statistical fluctuations of the autorod position etc.) the control rods are driven out the required amount (corresponding to a few cents, maximum 10 cents).
4. The measurement is ceased when the count-rate becomes too high (dead-time considerations).

The method of processing the raw data from the two techniques will now be described:

6.2.2.3. *Data Processing*

6.2.2.3.1. *Negative reactivities*

The processing of the raw data is performed by the specially written FORTRAN code IVK.FOR [6.34]. The code carries out the following tasks:

1. Reads in raw data, corrects for dead time losses, and applies the spatial correction factor defined in equation (6.28). It is probably sufficient to apply the factor after the rod-drop has occurred, however IVK applies the correction as a linearly increasing factor throughout the period of the drop as a means of improving the realism of the correction. It is not considered however that this makes a significant difference to the results. The rod drop characteristic had been measured previously using special position sensors with which it is possible to determine the position of the rod to within 0.5mm. The signal from this sensor was analyzed using a PC based LABVIEW application [6.43] to provide a rod characteristic curve and drop time. An example of a typical rod-drop curve, measured using this technique, and compared with the theoretical free-fall case is shown in Figure 6.12.
2. The code applies the integral method (equation (6.23)) using the drop time correction mentioned above.
3. The code calculates the differential reactivity (equation (6.21)) as a function of time through out the rod-drop

4. A user defined sliding average of the differential reactivity is performed to reduce the uncertainty of the integral rod worth

In a similar manner to ALPHUBEL, the IVK code has been extensively validated using simulated experiments [6.33, 6.34].

6.2.3.3.2. *Negative reactivities*

The processing of the raw data is performed by the specially written FORTRAN code PERIOD.FOR [6.41]. The code carries out the following tasks:

1. Reads in raw data, corrects for dead time losses
2. Makes a series of non-linear fits to the data to establish the best fit, i.e. the start channel of the fit is increased until the value of α and thus reactivity becomes independent of starting fit channel. This indicates that the negative components of the decay have disappeared; as have the spatial harmonics.

6.2.2.4. Uncertainties

6.2.2.4.1. *Negative Reactivities*

The uncertainty in rod drop measurements is notoriously difficult to estimate. The subject will not be treated here, instead, the reader may refer to [6.34], [6.1] and [6.11]

6.2.2.4.2. *Positive Reactivities*

The uncertainty in the reactivity obtained via stable period measurements arises from the statistical uncertainties in the measured data, appearing as an uncertainty on the fitted value of α_6 , and systematic uncertainties associated with the data used in the inhour equation to convert α_6 to reactivity. It will be noted that this situation is analogous to that for the Simmons-King technique, except, that due to the large differences in the magnitude of α used in the respective techniques (~ 0.007 in SP cf. ~ -50 in S-K) the importance of the various uncertainty components is somewhat different.

The statistical uncertainties can be reduced by increasing count rates and measuring times in individual measurements or by repeating measurements. The former method is limited by the particular properties of the counting system, namely dead-time and detector efficiency, and the latter method although effective, is expensive in time and effort. Using current techniques it was seen to be possible to determine α_6 to an accuracy of better than 0.5%.

Reductions in uncertainties associated with the use of a particular set of delayed neutron data in the processing of the measured parameters to yield the desired parameter, in this case reactivity, can only be achieved by using a better data set. This possibility is discussed briefly below.

Although the HTR-PROTEUS system contains two fissionable isotopes, the influence of the ^{238}U represents only a few percent of the total fission yield and has a correspondingly small influence on the delayed neutron properties of the system. Therefore, although the effective delayed neutron yields were calculated properly, taking into account the presence of the ^{238}U , using the perturbation theory code PERT-V, the uncertainties associated with these fractions, and the decay constants and their associated uncertainties were taken directly from the ^{235}U

isotopic data. To demonstrate the significance of this approximation, the effective and ²³⁵U isotopic group fractions are compared in Table 6.1 in Section 6.2.1.4 for the JEF 1 data.

The value of reduced generation time used in the analysis, was calculated using PERT-V but normalized to a value of Λ/β measured in each core. It will be seen below that this method is very insensitive to the value of Λ/β used and an uncertainty of 5% was therefore attributed to this parameter, although this is almost certainly an overestimate.

The inhour equation can be written as a sum of 7 terms, 1 prompt and 6 delayed

$$\rho = \underbrace{\Lambda^*}_{\text{(PROMPT) TERM-1}} + \underbrace{\frac{\alpha b_1}{\alpha + \lambda_1}}_{\text{TERM-2}} + \underbrace{\frac{\alpha b_2}{\alpha + \lambda_2}}_{\text{TERM-3}} + \underbrace{\frac{\alpha b_3}{\alpha + \lambda_3}}_{\text{TERM-4}} + \underbrace{\frac{\alpha b_4}{\alpha + \lambda_4}}_{\text{TERM-5}} + \underbrace{\frac{\alpha b_5}{\alpha + \lambda_5}}_{\text{TERM-6}} + \underbrace{\frac{\alpha b_6}{\alpha + \lambda_6}}_{\text{TERM-7}} \quad (6.30)$$

In which the subscripts relate to those appearing in Table 6.3. The contribution of each of these terms to the total reactivity is given in the table. These uncertainties were taken from a measurement of the worth of control rod 4 in the range 2500-2100mm inserted, in Core 5.

	Value (\$)	Uncertainty (\$)	Uncertainty (%)	Statistical Uncertainty Only (%)
TERM-1	0.00150	0.00014	9.3	
TERM-2	0.0140	0.0015	10.7	
TERM-3	0.0393	0.0018	4.6	
TERM-4	0.011	0.0015	13.6	
TERM-5	0.00926	0.00042	4.5	
TERM-6	0.00066	0.000084	12.7	
TERM-7	0.0000489	0.00001	20.4	
TOTAL	0.0758	0.0028	3.7	0.17

Table 6.3: Contribution of each of the terms of equation (6.30) with their corresponding uncertainty

Looking at the Table, the following comments should be made:

- the contribution of the prompt term to the reactivity is only some 2%
- the largest contributor to the reactivity is the second delayed group with more than 50% contribution. Fortunately, the uncertainties on the group 2 parameters are relatively low, which keeps down the uncertainty on the total reactivity
- the statistical uncertainty is only some 5% of the total uncertainty, indicating that further efforts to improve the measurement techniques are not necessary at present

6.2.3. Reactor Noise

Although it was mentioned, on the basis of a preliminary study made at the beginning of the program [6.44], that reactor noise was not chosen as one of the main techniques to be used on HTR-PROTEUS, there was some interest shown amongst some of the participating organizations, namely the Kurchatov Institute in Moscow, and the Technical University of Delft in the Netherlands, in applying noise techniques to PROTEUS. Detailed descriptions of these measurements are provided in [6.2, 6.45, 6.46]. Some comments on the results of these studies are given in the corresponding part of Section 7.

6.3. KINETIC PARAMETER (β/Λ)

6.3.1. Introduction

As the methods chosen to measure reactivity effects in HTR-PROTEUS are based upon kinetics techniques, which themselves rely upon accurate estimates of the generation time (Λ) and the effective delayed neutron fraction (β_{eff}) a measurement of these two parameters was an important accompaniment to the main measurement program. Furthermore, the validation of reactor physics codes' ability to accurately predict β_{eff} and Λ is useful in the broader context of reactor transient analysis in which the margin to prompt criticality and the prompt reproduction time are deciding factors in the severity of potential accidents.

Unfortunately, no practical technique is available for the direct measurement of Λ and, although the measurement of β_{eff} in isolation is in principle possible, the techniques necessary are somewhat involved if a reasonable accuracy is required [6.47]. One alternative is to measure the prompt neutron decay constant at critical and to convert this to the ratio ($\beta_{\text{eff}}/\Lambda$) via a calculated correction factor. This approach has the advantage, as will be demonstrated, that it lends itself to a relatively clean and precise measurement but with the obvious disadvantage that observed calculation-to-experiment (C/E) discrepancies cannot easily be ascribed to either β_{eff} or Λ .

Measurements of $\beta_{\text{eff}}/\Lambda$ have been reported in the literature for a wide range of systems, mostly, as it happens, by Japanese groups. For graphite moderated systems, results have been published both for the Semi-Homogeneous Experiment (SHE) and for its successor the Very High Temperature Reactor Critical (VHTRC), at JAERI. In SHE, which was fueled mainly with 20% enriched uranium, both pulsed-neutron source (PNS) and neutron noise type measurements were carried out. In the latter type of measurement, the "polarity correlation" technique [6.48] was used to measure α at various states of subcriticality (including critical). The PNS measurement followed along similar lines except that in this case no measurement of α at critical could be made and an extrapolation technique was adopted. It was recognized in this work that the variation of α with reactivity is not linear in such slow systems, due to so-called "delayed neutron contamination" of the prompt mode, and consequently the measured data was fitted instead to a simplified form of the inhour equation to yield α at critical. The results of both PNS and noise measurements in SHE have subsequently been compared with calculations made with the CITATION diffusion theory code which forms part of the SRAC system [6.49]. The calculations were made in 2-D and 24 energy groups and cross sections were obtained from the ENDF-B/IV data set. An average C/E of 1.03 ± 0.02 was observed. The authors comment that an improvement of $\sim 1\%$ in their calculations could be made by using a prompt flux distribution instead of a static one.

In the VHTRC-1 core, which was fueled exclusively with 4% enriched uranium, PNS measurements were also used to measure $\beta_{\text{eff}}/\Lambda$ [6.50]. The results are compared to 3-D CITATION calculations in 24 groups and a C/E of 1.13 ± 0.02 is reported.

As far as other types of system are concerned, PNS measurements were also used in the Japan Materials Testing Reactor Critical (JMTRC) facility, a light water moderated system fueled both with high and medium enriched uranium (HEU, MEU) [6.51]. In this case, α is of the order of 100s^{-1} at critical, the delayed neutron contamination mentioned above can be neglected, and a linear fit to the reactivity vs. α relationship is appropriate. However, again using CITATION in 3-D (this time in 4 energy groups) C/Es of 1.13 and 1.15 respectively were observed in the MEU and HEU systems indicating, in this case at least, that the form of the fit function is not the only major source of error.

Finally, the Feynmann- α method was used to measure $\beta_{\text{eff}}/\Lambda$ in the 93.1% enriched Kyoto University Critical Assembly [6.52]. Using CITATION in 52 groups, C/E values of between 1.1 and 1.2 were observed with quoted uncertainties of some 2-3%.

The fact that C/E discrepancies are observed for independent measurements in a wide range of systems provided an extra incentive to carry out measurements in PROTEUS. It will be seen that the particular properties of the current PROTEUS configurations, namely undermoderated cores with consequently large reflector effects result in relatively long generation times and that these conditions constitute a most stringent test of the measurement techniques. Particular emphasis is therefore given to the scrutiny of the measurement analysis procedure as a means of eliminating the possibility of systematic measurement errors.

6.3.2. Theory of the Analysis

The theory is again based upon the inhour equation with 6 delayed neutron groups:

$$\rho(\$) = \alpha\Lambda^* + \sum_{i=1}^6 \frac{b_i\alpha}{\alpha + \lambda_i} \quad (6.31)$$

in which all symbols have already been defined

In a critical system, $\rho(\$) \equiv 0$ and hence:

$$\frac{\alpha^c \Lambda^c}{\beta_{\text{eff}}^c} = - \sum_{i=1}^6 \frac{b_i \alpha^c}{\alpha^c + \lambda_i} \quad (6.32)$$

in which the superscript 'c' indicates the critical state.

Re-arranging equation (6.32) we have:

$$\frac{\beta_{\text{eff}}^c}{\Lambda^c} = - \frac{1}{f^c} \cdot \alpha^c \quad (6.33)$$

in which:

$$f^c = \sum_{i=1}^6 \frac{b_i \alpha^c}{\alpha^c + \lambda_i} \quad (6.34)$$

Equation (6.33) indicates that, having measured α^c it is possible, with the application of a modest correction factor, which itself is dependent upon α^c , to derive a value for $\beta_{eff}^c / \Lambda^c$. However, in systems with long generation times ($\sim 10^{-3}$ s) such as the current PROTEUS configurations, the direct measurement of α^c is hindered by virtue of the fact that α^c is similar in magnitude to the shortest lived delayed neutron precursor λ_1 (a value of $-3.87s^{-1}$ was used in this work. The difficulties in isolating α^c from the delayed background are, for this reason, much greater in graphite systems. In order to overcome these difficulties, it is common to measure α at several different, well known, states of subcriticality and to extrapolate a fit to the measured points to $\rho = 0$ and hence $\alpha = \alpha^c$. Looking at equation (6.31), ρ is clearly a non-linear function of α . However, in the special case of systems with prompt decay constants having magnitudes much greater than the λ_i , as in water moderated or very subcritical systems then:

$$\sum_{i=1}^6 \frac{b_i \alpha}{\alpha + \lambda_i} \xrightarrow{\alpha \gg \lambda_i} 1 \quad (6.35)$$

and equation (6.31) tends to linearity - the so-called *prompt approximation*. However, for the reasons discussed above, in the case of measurements in the current PROTEUS configurations the influence of the summation term in (6.31) is significant and must be taken into account. Furthermore, equation (6.31) does not automatically take into account the fact that, in changing the reactivity of the system, the value of Λ and to a lesser extent β_{eff} will also change. This effect will also contribute to the non-linearity in the measured relationship between ρ and α .

As a means of quantifying the typical magnitudes of these non-linearity effects, such that the best method of measurement analysis could be chosen, a calculational study has been carried out, taking the form of a simulation of the $\beta_{eff}^c / \Lambda^c$ experiment, using the MICROX / TWODANT / PERT-V route. The following approach was taken:

1. Using forward and adjoint fluxes derived from a TWODANT model representation of HTR PROTEUS Core 1, Λ and β_{eff} were calculated, using PERT-V, for various subcritical states in the range 0 to -1.3\$.
2. The values of Λ and β_{eff} thus derived, together with the TWODANT value of $k_{effective}$, were used to calculate a value of α , the most negative root of equation (6.33), for each subcritical state.

A plot, versus ρ , of these values of α serves to indicate the degree of non-linearity inherent in the ρ/α relationship, both as a result of the form of the inhour equation and of the dependence of Λ and β_{eff} on ρ . Furthermore, the extrapolation to α^c of various fits to these data can then be compared with the "true" value, calculated directly from a TWODANT model with $\rho = 0$, and used to find the fit function which provides the most accurate "measured" value of α^c . A typical measurement range is $1.3\$\leq\rho\leq-0.26\$\$ comprising about 5 measured points. By way of example, 3 different fits were typically made to the data

FIT 1 Linear:

$$\rho = A + B\alpha$$

FIT 2 Inhour equation with $\Lambda/\beta \neq f(\alpha)$

$$\rho = A\alpha + \sum_{i=1}^6 \frac{b_i\alpha}{\alpha + \lambda_i}$$

FIT 3. Inhour equation with $\Lambda/\beta = f(\alpha)$

$$\rho = (A + B\alpha)\alpha + \sum_{i=1}^6 \frac{b_i\alpha}{\alpha + \lambda_i}$$

Qualitatively, the results show that, although most of the fits seem to represent the measured points very well, the extrapolations to $\rho = 0$, $\alpha = \alpha^c$ show a relatively large spread.

Fit Type ^a	χ^2	α_0^c	f^c	$\beta_{eff}^c / \Lambda^c$	% error in $\beta_{eff}^c / \Lambda^c$
FIT 1	8x10 ⁻⁵	-5.2200	1.1537	4.5246	-5.65
FIT 2	2x10 ⁻⁴	-5.5042	1.1356	4.8469	1.07
FIT 3	8x10 ⁻⁷	-5.4451	1.1389	4.7810	-0.3
"True"		-5.4584	1.1382	4.7956	0

a - see definitions in text

Table 6.4: Results of the Numeric Simulation of the $\beta_{eff}^c / \Lambda^c$ Experiment

Table 6.4 summarizes the numeric results of these fits from which the following observations can be made:

- Looking at the χ^2 values for the individual fits, the best result is obtained with a curve having the form of the inhour equation with a Λ/β value which itself is a function of α (referred to as FIT 3 from now on). However, having previously mentioned that the curvature in the ρ vs. α relationship is most severe close to critical, this goodness of fit is not necessarily the best measure of the most accurate extrapolation to α^c
- Comparing the extrapolated values of α^c with the "true" value shown in the bottom row of the table, the linear fit (FIT 1) gives the worst result with a 4.4% overestimate, whereas FIT 3 provides the best result with only a 0.24% overestimation.
- The three extrapolations to α^c were used to calculate the factor f^c which in turn was used to calculate values of $\beta_{eff}^c / \Lambda^c$. Because f^c depends on α^c , any error in α^c leads to a larger error in $\beta_{eff}^c / \Lambda^c$. Consequently, the final column in Table 6.8 indicates that, in using a linear fit we should expect systematic errors in our measured value of $\beta_{eff}^c / \Lambda^c$ of the order of 5.7%.

In conclusion:

The use of a fit function with the form of the inhour equation with a value of Λ/β which itself is a linear function of α is the preferred approach.

6.3.3. Experimental Methods

The experimental procedure and apparatus is practically identical to that described for the PNS measurements in Section 6.2.1.2. Because the prompt decay constant is a global parameter, its measurement is not position sensitive and it is only important to choose the

source-detector distance so as to minimize source harmonic and dead-time effects but also as to optimize counting statistics. This spatial independence was repeatedly checked and confirmed during the course of the measurements. To summarize:

For the measurements in each core configuration, the first step was to establish a critical balance with the PNS and other instrumentation in place and the reactor start-up sources withdrawn. The reactor was then shutdown to the required subcriticality by means of the control rods, and, after a waiting time sufficient to allow delayed neutron effects to subside, the PNS was activated. After a further waiting period of ~15 minutes to allow an equilibrium flux distribution to be established, counting could begin. Between 200 and 800 pulses were sufficient to obtain satisfactory counting statistics. For each core, a range of different subcritical states between -1.0 and -0.13\$ were measured. The reactivity scale was determined by means of careful measurement of the differential worth curves of each of the 4 control rods via stable period measurements (see Section 6.2.2.1.2.). If the worth of the control rods were a linear function of their insertion, it would be sufficient to plot each measured α against the corresponding control rod insertion (in mm for example) and to extrapolate the resulting curve to the critical rod insertion to obtain α^c . However, it is generally not the case that the rods have a linear response and thus it is necessary to calibrate the rods in terms of reactivity units, traditionally β_{eff} . Furthermore, as a by-product of the measurement of α , it is possible, with the use of a calculated value for the generation time Λ , to derive a quasi independent estimate of the reactivity at each state via a Simmons-King analysis (Section 6.2.1.1.1.) of the PNS measurements. This provides a very convenient check of our rod calibration.

6.3.4. Data Processing

The raw data was analyzed with the specially developed ALPHUBEL code (described in Section 6.2.1.3.), which was developed to isolate the prompt response from PNS measurements, make a fit to this response to derive a value for α and thus to derive reactivity via several different techniques. As described in Section 6.2.1.3, in order to eliminate the effect of prompt harmonics from the responses, the "tornado plot" approach, [6.19], was adopted.

Having derived typically 4 or 5 values of α for a range of subcriticalities, fits of the form FIT3 and FIT1 were made to the data. The derived functions were then used to determine α^c and hence $\beta_{eff}^c / \Lambda^c$

It should be pointed out that in configurations such as Core 5 in which α is particularly close to λ_1 , the curvature of equation (6.31) is significant (see Section 7.5). This causes a particular sensitivity to the choice of the delayed neutron data used in the analysis.

6.3.5. Uncertainties

Similar comments apply, as were made for the α uncertainties in the PNS techniques. However, further allowances must be made for the uncertainties associated with the fit of ρ versus α and for the conversion of α^c to β^c/Λ^c

6.4. REACTION-RATE MEASUREMENTS

Alongside critical loadings and reactivity worths, the third main theme of the HTR-PROTEUS experiments was the investigation of the individual neutron-balance components, including

fission and capture rates and leakage/reflector effects. What follows is a very brief summary of the reaction rate measurements, again a very detailed description, albeit in the German language, may be found in [6.3]

Although a good deal of experience was already available in PROTEUS in the field of reaction-rate measurements [6.53] there were some aspects peculiar to a LEU-HTR system which had not previously been addressed. In particular, the measurement of the capture rate in ^{238}U (C8), in doubly heterogeneous fuels requires particular attention with regard to the reconstruction of the fuel particle geometry to account for resonance self-shielding effects. In this context, novel techniques were developed involving the use of the fuel particles themselves as activation foils thus avoiding the need for self-shielding correction factors. This technique will be described later in this section.

One of the main incentives for the use of deterministic pebble loadings was the experimental convenience with respect to the measurement of these neutron balance components. In particular, the deterministic loadings allow:

- the measurement of axial and radial reaction-rate traverses in the channels between the pebbles in both hexagonal close packed (HCP) and columnar hexagonal or point-on-point (POP) using miniature fission chambers and activation foils.
- the measurement of the distribution of reaction rates within the pebbles themselves. Since this must be done in the core center to be away from the disturbing influences of the reflector and cavity, this measurement can only be applied in POP cores. Techniques used include the activation of U-metal, U/Al and fuel matrix foils.
- axial reaction-rate distributions by means of γ -scanning a column of pebbles in the POP configurations.
- the measurement of reaction rates and reaction-rate ratios in the fuel matrix of pebbles in the core center of POP cores using foil activation and γ -scanning

6.4.1. Description of the Apparatus: Foils, Particles, Pellets, Deposits, Pebbles and Chambers

6.4.1.1. Fission Chambers

Miniature ($\sim 4\text{mm}$ \varnothing) fission chambers containing deposits of ^{235}U , ^{238}U , ^{237}Np and ^{239}Pu were used to measure relative reaction-rate traverses in the axial channels between the pebbles.

6.4.1.2. Foils

Fission rates in ^{235}U (F5) were measured with Uranium/Aluminum (U/Al) foils. These foils are 93% enriched in ^{235}U and are coated in a layer of Nickel to avoid contamination. Two sizes of foil, having diameters of 6.7mm and 8.46mm were used.

Fission and capture rates in ^{238}U (F8 and C8) were measured with metallic, depleted-uranium foils (0.0378%). Again, two foil diameters were used, namely 6.7mm and 8.46mm

6.4.1.3. Particle Foils and Particles

Special “foils” consisting of fuel matrix material were also used. Two types were used, one type was fabricated in PSI, the other in the Kurchatov Institute in Moscow.

The Swiss type were machined from actual LEU fuel pebbles and although this had the advantage that the ^{235}U enrichment was known to be the same as that in the core, there was the disadvantage that no information was available on the distribution of particles in the foil and furthermore there was some doubt as to the mechanical strength of the foil and whether particles could be lost from the outside surface.

The Russian type of particle foils were constructed specially and possessed therefore a well known particle density and distribution. These foils were available in two enrichments (0.72% and 16.7%) and various carbon-to-uranium (C/U) ratios.

In addition, individual particles were also fabricated in Moscow. These had again enrichments of 0.72% and 16.7% and could be placed in graphite foil holders for use as activation “foils” within fuel pebbles. **None of the Russian particles were coated**

6.4.1.4. Demountable Fission Chambers and Deposits

Absolutely calibrated deposits were used in demountable fission chambers (diameter $\approx 60\text{mm}$) as a reference source in the determination of absolute fission rates. The deposits consist of an α -active, fissionable material, either ^{235}U or ^{238}U depending on the type of measurement. The α -activity is used to calibrate the deposits. The construction and function of the demountable fission chamber is described in [6.53]. The principle of the chamber is that similar foils can be placed in a pebble at the core center and also within the demountable fission chamber which is situated at a suitable distance so as not to perturb the reaction rates there. The reaction rate measured in the core center may then be converted to an absolute rate via the fission product gamma activities of the two activation-foils and the count rate of the fission chamber.

6.4.1.5. Measurement Pebbles and Pellets

In order that the foils described above could be located within the fueled region, special pebbles had to be fabricated.

Through the center of each of these special pebbles, a cylindrical channel of 10mm diameter was machined. This channel was used to locate measurement pellets and foils. The measurement pellets act as filler pieces with which to locate the foils precisely within the pebble and were machined from LEU fuel matrix material. The ends of some of the measurement pellets contain slight depressions in which the foils can be located. The channel can be sealed by means of a threaded cap, made from graphite. The pellets can also be used as detectors in the measurement of F_{tot}

6.4.2. Reaction Rate Distributions in Core

These distributions are, in the main, relative ones. The main method used in axial traverses is the miniature fission-chamber, but foils are also used as a means of reducing systematic errors and also for radial traverses. It is possible, by virtue of channels in the upper and lower axial reflectors to measure over the total height of the system. In the radial direction, there are some access possibilities through the radial reflector, but in general, radial traverses have only been made in the core region. A few azimuthal traverses in the radial reflector have also been made with foils. A further alternative for axial traverses is the γ -scanning of individual pebbles. The application of the three techniques will now be described.

6.4.2.1. Fission Chambers

As was mentioned above, the miniature fission chambers are small enough to pass between the pebbles in both HCP and POP configurations. The fission chamber position was adjusted remotely between measurements with a typical interval of 5cm. Reactivity was maintained constant by the autorod as the chamber was withdrawn from the core. The typical sensitivities of the chambers dictated operating fluxes of some $10^8 \text{ n.cm}^{-2}.\text{s}^{-1}$. For the measurements of fast reaction rates (e.g. F8) the chambers were shielded with cadmium to eliminate the need to correct for the presence of trace quantities of thermally fissionable nuclides. Because the measurements are relative ones, some systematic errors cancel, however the following global uncertainties have to be considered:

- statistical errors (counting statistics): due to dead time considerations and the large variation of reaction rates across the system, especially for fast reaction rates, it is not possible to achieve optimum count rates throughout the traverse. In certain regions, namely the outer reflector regions, this leads to low count rates and large statistical errors.
- radial position: the outer diameter of the fission chambers is somewhat smaller than the size of the channels in the pebble bed. This leads to an uncertainty in the radial position of the fission chamber in the core. Since the channels in the upper and lower reflector are significantly wider than those in the core, the uncertainty in these regions (and of course in the cavity region) is somewhat larger
- axial position: due to the light weight of the chamber the cable is not fully extended and thus similar positions on the oscillator can lead to slightly different axial positions of the detector. This leads to a further uncertainty which must be accounted for.
- discrimination: of the fission chamber spectrum
- perturbation by fission chamber:

The magnitude of these uncertainties, for fast and thermal reaction rate measurements are summarized in tables 6.5 and 6.6. As certain errors are seen to be dependent on the position of the measurement, it was convenient to divide the system into 4 distinct regions.

Error	lower axial reflector	core	cavity	upper axial reflector
Statistical	0.3-5.0%	0.3-0.5%	0.5%	0.5-5%
Systematic				
radial position	0.2%	0.1%	0.2%	0.2%
axial position	0.2%	0.2%	0.2%	0.2%
discriminator	0.2%	0.2%	0.2%	0.2%
perturbation by chamber	0.5%	0.5%	0.5%	0.5%
Total	0.7-5.2%	0.6-0.8%	0.8%	0.8-5.2%

Table 6.5: Error estimate for F5 Reaction Rates Measured with a Miniature Fission Chamber

Error	lower axial reflector	core	cavity	upper axial reflector
statistical	1.0-10.0%	0.5-1.0%	1.0-2.0%	2.0-10.0%
systematic				
radial position	0.2%	0.1%	0.2%	0.2%
axial position	0.2%	0.2%	0.2%	0.2%
discriminator	0.5%	0.5%	0.5%	0.5%
perturbation by chamber	0.5%	0.5%	0.5%	0.5%
Total	1.3-10.1%	0.9-1.3%	1.3-2.2%	2.2-10.1%

Table 6.6: Error Estimate for F8 and F7 Reaction Rates Measured with a Miniature Fission Chamber

6.4.2.2. Foils

It was mentioned above that radial and axial reaction rates were measured with activation foils, U/Al foils for F5 and metallic uranium foils for F8. The foils were attached to special aluminum rods and introduced between the pebbles. As in the fission chamber measurements, the foils were shielded with cadmium for the F8 measurements. The measurement uncertainties can be summarized as follows:

- statistical errors (counting statistics):
- radial position: because the aluminum rod is not the same size or shape as the channels between the pebbles, the position of the foils cannot be exactly determined
- axial position: because the foils occupy specially machined depressions in the aluminum, the uncertainty in the axial position of the foils is smaller
- intercalibration (U/Al foils): the foils were intercalibrated in the thermal column of PROTEUS
- foil weight (U-metal foils): these foils are not nickel coated and so their mass is a good indication of the heavy metal content
- time correction

The magnitude of these various uncertainties is summarized in the Table 6.7.

Error	F5	F8
statistical	0.3%	0.5-1.0%
systematic		
radial position	0.2%	0.2%
axial position	0.1%	0.1%
intercalibration	0.3-0.5%	-
foil weight		0.1%
Total	0.5-0.7%	0.6-1.3%

Table 6.7: Error estimate for F5 and F8 Reaction Rates Measured with Activation Foils (in Core)

6.4.2.3. γ -Scanning

The direct gamma scanning of activated pebbles was used as an alternative to foil techniques. The method is described in [6.3].

6.4.3. Reaction Rate Distributions in Pebbles

Methods to measure within pebble reaction rate distributions were also developed, these are also described in great detail in [6.3]

6.4.4. Reaction Rate Ratios

The reaction rate ratios F8/F5 and C8/F5 were measured with a combined foil/fission chamber technique. The ratio C8/F_{tot} was determined by means of the γ lines of ^{293}Np and other fission products. Pellets, foils, particles and whole pebbles were used as detection media.

6.4.4.1. Determination of F8/F5

For the measurement of the ratio F8/F5, the demountable fission chamber was used, with absolutely calibrated deposits and intercalibrated foils. By comparison of the fission product activity of the foils in the fission chamber and the foils in fuel pebbles, the fission rate of the fission chamber can be converted to an unperturbed fission rate in the fuel. The equation for the determination of F8/F5 can be written as follows:

$$\frac{F8}{F5} = \frac{F8(D)}{F5(D)} \cdot \frac{F5(F, SpK)}{F5(F, Kugel)} \cdot \frac{F8(F, Kugel)}{F8(F, SpK)} \cdot FD \cdot FF \quad (6.36)$$

in which:

F8(D) = absolute F8 of deposit

F5(D) = absolute F5 of deposit

F5(F,SpK) = fission product activity of the U/Al foil in the fission chamber

F5(F,Kugel) = fission product activity of the U/Al foil in the fuel pebble

F8(F,SpK) = fission product activity of the U-metal foil in the fission chamber

F8(F,Kugel) = fission product activity of the U-metal foil in the fuel pebble

FD = correction factor for the deposit

FF = correction factor for the foils

The correction factors FD and FF comprise the following effects

Deposits (FD)

- extrapolation to zero
- fission product self-absorption: calculated and measured with a special fission chamber
- axial flux gradient: measured via comparison of fission rates of two deposits built simultaneously into the fission chamber
- Number of nuclides: determined via measurement of the emitted α particles
- Foreign nuclides: ^{235}U deposits contain 6% ^{238}U , ^{238}U deposits contain 0.0378% ^{235}U
- Dead-time: 0.7 μs , checked routinely with standard sources

Foils (FF)

- Foreign nuclides: U-metal foils contain 0.0378% ^{235}U
- Intercalibration

- Foil weight
- Foil effect: from the activation of irradiated single foils and packets of 2 foils, an extrapolation to an infinitely thin foil was made

Error	F5	F8
statistical	0.5%	0.5%
systematic		
<u>deposit</u>		
ETZ	0.1%	0.1%
Self-absorption	0.1%	0.3%
Flux-gradient (axial)	0.1%	0.1%
Nuclide number	0.5%	0.9%
Foreign nuclides	0.1%	0.5-2.5%
Dead-time	0.1%	-
<u>foils</u>		
Intrcalibration	0.3-0.5%	-
Foil weight	-	0.1%
Foil effect	0.3%	0.3%
Total	0.9-1.0%	1.2-2.7%

Table 6.8: Error estimate for F5 and F8 Reaction Rates Measured with Foils and Deposits

6.4.4.2. Determination of C8/F5

The capture rate C8 was measured via the 278keV γ -line from the β^- decay of ^{239}Np . The γ spectra were measured using high purity germanium detectors whose efficiency was determined using ^{243}Am Sources. The general relationship can be written as follows:

$$\frac{C8}{F5} = \frac{A_8^\infty}{F5(D)} \cdot \frac{F5(F, SpK)}{F5(F, Kugel)} \cdot FF \cdot FC \quad (6.37)$$

in which:

A_8^∞ = the saturation activity of ^{239}Np

FC represents further corrections for the determination of C8. These comprise:

- Foil weight
- Equivalent foil thickness: this accounts for the different resonance shielding in foils and particles. The procedure described in [6.54] was adopted.
- γ self absorption in a foil: this correction was taken into account using an experimentally determined mass-absorption coefficient for the 278 keV line [6.55,6.56]

- Half-life: consideration of the errors in the half-lives for ^{239}U and ^{239}Np which are used for the determination of the saturation activity
- Efficiency: uncertainty in the activity of the source
- Pile-up: Losses in the 278 keV photopeak due to pile-up of pulses in the main amplifier
- Geometry effects: ^{243}Am sources with diameters of 6.7mm and 12.1mm are available whereas foils are also used with a diameter of 8.46mm
The ^{243}Am sources with different diameters are located in different types of holders

The magnitude of these various corrections is listed in Table 6.9.

Error	C8
statistical	0.3%
systematic	
<u>foils</u>	
Foil weight	0.1%
Equivalent foil thickness	0.5%
Self absorption	0.5%
Time correction, half-life	0.1%
<u>detector system</u>	
Efficiency calibration	0.4%
Pile-up, background	0.2%
Geometry	0.2%
Total	0.9%

Table 6.9: Error estimate for C8 Reaction Rates Measured with Foils

6.4.4.3. Determination of C8/ F_{tot}

The ratio C8/ F_{tot} was measured by means of γ spectrometry of LEU-HTR pellets, particle foils and whole fuel pebbles. F_{tot} was determined from various γ lines such as the 293 keV line of ^{143}Ce and the 1596 keV line of ^{140}La . C8 was determined via the 278 keV photopeak of ^{239}Np . C8/ F_{tot} can be determined from the following equation:

$$\frac{\text{C8}}{F_{\text{tot}}} = \frac{A_8^\infty}{A_{\text{tot}}^\infty} \cdot \frac{SA_{\text{tot}}}{SA_8} \cdot \frac{E_{\text{tot}}}{E_8} \cdot \frac{EW_{\text{tot}}}{EW_8} \cdot SP \quad (6.38)$$

in which:

A_8^∞ = saturation activity of ^{239}Np

A_{tot}^∞ = saturation activity of the specific fission product

SA_{tot} = γ -self absorption of the fission product in the sample

SA_8 = γ -self absorption of the ^{239}Np in the sample

E_{tot} = detector efficiency for energy of the observed fission product

E_8 = detector efficiency for the observed energy of the ^{239}Np

EW_{tot} = emission probability of the γ quanta of the fission product

EW_8 = emission probability of the γ quanta of the ^{239}Np

SP = fission product yield

The uncertainties for the emission probabilities and for the fission product yields were taken from [6.57] and [6.58] respectively. The errors for the γ -self absorption of the various nuclides were calculated and are to be found in [6.59]. Further corrections, for the detection system, have to be taken into account:

- Efficiency calibration: The calibration of the detectors was carried out with calibration sources having a diameter of ca. 3mm
- Pile-up, dead time: Losses caused by pile-up and dead time in the main amplifier and also dead time in the ADC
- Geometry differences: The calibration sources have a diameter of 3mm whereas for instance the LEU measurement pellets have a diameter of ca. 10mm

The emission probability of the 278 keV photopeak of ^{239}Np is the largest source of error. This source can be ignored, if the efficiency calibration is carried out with an ^{243}Am source, because then the detector is calibrated with the same nuclide. In this case however, the geometry correction becomes larger because firstly the ^{243}Am source does not fit into the same holder as the measurement pellets and foils and secondly the diameter is different. The estimated errors for $C8/F_{tot}$ are listed in Table 6.10.

Error	F_{tot}	F_{tot}	C8
	^{143}Ce (293 keV)	^{140}La (1596 keV)	^{293}Np (278 keV)
statistical	0.3%	0.3%	0.5%
systematic			
<u>nuclide</u>			
Emission probability	0.9%	0.1%	0.9%
Fission Product yield	0.8%	1.0%	-
Half Life	0.1%	0.1%	0.1%
γ -self absorption	0.1%	0.2-0.4%	-
<u>detector system</u>			
Efficiency calibration	0.7%	1.0%	-
Pile-up, background	0.1%	0.1%	0.1%
Geometry	0.1%	0.1%	0.1-0.5%
Total	1.4%	1.5%	1.0-0.7%

Table 6.10: Error Estimates for the Fission Rates F_{tot} and C8 Measured with LEU-HTR Pellets and Particle Foils

6.5. GRAPHITE ABSORPTION MEASUREMENTS

6.5.1. Introduction

One of the common features of the HTR-PROTEUS configurations was a large reflector importance and a subsequently high sensitivity to the presence of poisons in the reflector graphite (see [6.60] in which values of ≈ 3 \$/mbarn for the reflector graphite and ≈ 1 \$/mbarn for the core graphite are quoted for graphite with a nominal "clean" value of 3.4mb). The accurate determination of this parameter was therefore vital for code validation via measurements in PROTEUS and it was therefore considered appropriate to include a description of the measurement of the parameter in HTR-PROTEUS in this section on measurement techniques, although it does not represent one of the required parameters of the program as such.

The effective absorption of graphite can be measured in several ways:

1. Chemical Analysis Yields elemental concentrations in small samples which must be converted to absorption via tabulated cross sections. It is not guaranteed that such an analysis will detect intergranular gaseous components, which can be important.
2. Reactor-Based Measurements These give a direct measurement of the effective absorption cross-section of small samples via comparison with standard absorbers.
3. Decay-constant Measurements These give a direct indication of the **global** effective absorption in a system.

All three methods were ultimately used in the investigation of the HTR-PROTEUS graphite properties. All measurements and results are reported adequately elsewhere [6.60, 6.61]

6.5.2. The HTR-PROTEUS Graphite

The HTR PROTEUS system consisted of graphite from several different sources, these sources being summarized in Table 6.11. It was expected that the data for the newer graphite be fairly reliable, but the older graphite, which formed the majority of the system, was of more concern. It is now more than 25 years old, and has been often handled during this time.

GRAPHITE TYPE	OCCURENCE	DENSITY (g.cm ⁻³)	σ_a (mbarn.atom ⁻¹)
Old graphite remaining from previous experiments	Majority of system	1.76±0.01 1	3.785±0.3 ¹
New graphite for HTR PROTEUS - Batch 1	1. Central part bottom axial reflector 2. Central part top axial reflector 3. Filler rods for ≈ 50% "C-Driver" channels (inner channels) 4. Top 12cm of radial reflector 5. Filler pieces to adjust cavity shape for required geometry	1.75±0.00 7 ²	3.77±0.09 ²
New graphite for HTR PROTEUS - Batch 2	1. Filler rods for ≈ 50% "C-Driver" channels (outer channels) 2. Filler pieces for old ZEBRA rod channels 3. Alternative central part of bottom reflector with longitudinal channel to allow axial traverses.	1.78 ³	4.08 ³
Moderator pebbles	Core	1.68±0.03 4	4.79 ⁴
Fuel pebbles	Core	1.73 ⁴	0.3829 ⁴ ppm B

1 Reactor-based measurements reported in N.R.E PROTEUS Construction Manual Section A

2 Reactor-based measurements SERS Test Certificates 25.01.91 and 10.10.91

3 Reactor-based measurements SERS Test Certificate 7.01.93

4 Chemical analyses HOBEG GmbH Test Certificates for fuel and moderator pebbles.

Table 6.11: Summary of Reactor Graphite in HTR-PROTEUS

REFERENCES

- [6.1] ROSSELET, M., "Reactivity Measurements and their Interpretation in Systems with Large Spatial Effects," Thesis Nr. 1930, Swiss Federal Institute of Technology, Lausanne (1999)
- [6.2] WALLERBOS, E.J.M., "Reactivity Effects in a Pebble Bed Type Nuclear Reactor," Doctoral Thesis (1998) University of Delft, Netherlands
- [6.3] KOEBERL, O., "Experimentelle Neutronenbilanzuntersuchungen zum Wassereinbruch in einen Hochtemperaturreaktor mit niedrig angereichertem Uranbrennstoff," Thesis Nr. 1803, Swiss Federal Institute of Technology, Lausanne (1998)
- [6.4] WILLIAMS, T., "HTR PROTEUS Core 1: Approach to Critical and Measurement of Safety Parameters", PSI Internal Report TM-41-92-38, Nov. 1992.
- [6.5] SEILER, R., BOURQUIN, P., "Betriebsvorschriften HTR-PROTEUS", PSI Internal Report AW-41-91-01
- [6.6] WILLIAMS, T., "HTR-PROTEUS CORE 1: Reactivity Corrections for the Critical Balance", PSI Internal Report TM-41-93-20, Oct. 1993
- [6.7] BRANDES, S., DAOUD, H., SCHMID, U., "Core Physics Tests of Thorium High-Temperature Reactor Pebble-Bed Core at Zero Power," Nucl. Sci. & Eng., 97, 89-95, (1987)
- [6.8] WILLIAMS, T., CHAWLA, R., "Intercomparison of Rod Worth Measurement Techniques in a LEU HTR Assembly," Proc. Int. Conf. on Reactor Physics and Reactor Computations, "Jan 23-26, 1994, Tel Aviv
- [6.9] WILLIAMS, T., "Reactivity Measurements in VHTRC and KAHTER", PSI Internal Report TM-41-91-08, April 1991
- [6.10] ROSSELET, M., WILLIAMS, T. and CHAWLA R., "Subcriticality Measurements Using an Epithermal Pulsed-Neutron Source Technique in Pebble Bed HTR Configurations," Ann. Nucl. Energy, **25**, No. 4-5, 285 (1998)
- [6.11] ROSSELET, M., CHAWLA, R. and WILLIAMS, T., "Epithermal Inverse Kinetic Measurements and Their Interpretation Using a Two Group Model," Nucl. Sci. And Eng., 135 (2000)
- [6.12] WILLIAMS, T., "Preliminary Investigation of Pulsed Neutron Measurements on HTR-PROTEUS," PSI Internal Report TM-41-90-28, Aug. 1990
- [6.13] SJÖSTRAND, N.G., "Measurements on a Subcritical Reactor using a Pulsed Neutron Source," Arkiv for Fysik, **11**, 233, (1956)
- [6.14] SIMMONS, B. E., KING, J. S., "A Pulsed-neutron Technique for Reactivity Determination," Nucl. Sci. & Eng., **3**, 595, (1958).
- [6.15] GOZANI, T., "A Modified Procedure for the Evaluation of Pulsed Source Experiments in Subcritical Reactors," Nukleonik, **4**, 348, (1962)
- [6.16] GARELIS, E., RUSSEL Jr., J.L., "Theory of Pulsed Neutron Source Measurements," Nucl. Sci. & Eng., **16**, 263, (1963),

- [6.17] KANEKO, Y., "Integral Versions of Some Kinetic Experiments for Determining Large Negative Reactivity of Reactor," *J. Nucl. Sci & Technol.*, **12** (7), 402 (1975)
- [6.18] BROWN, J.R., PRESKITT, C.A., NEPHEW, E.A., VAN HOWE, K.R., "Interpretation of Pulsed-source Experiments in the Peach Bottom HTGR," *Nucl. Sci. & Eng.*, **29**, 283, (1967)
- [6.19] BROWN, J.R., PFEIFFER, W., MARSHALL, A.C., "Analysis and Results of Pulsed-neutron Experiments Performed on the Fort St. Vrain High Temperature Gas-Cooled Reactor," *Nucl. Tech.*, **27**, 352, (1975)
- [6.20] WILLIAMS, T., "The Calculation of Kinetics Data for Use in the Simmons-King Analysis of Pulsed Neutron Measurements," PSI Internal report TM-41-93-36, June 1994
- [6.21] KEEPIN, G. R., "Physics of Nuclear Kinetics," Addison-Wesley Publishing Co., Reading, Massachusetts, (1965)
- [6.22] AKINO, F., YASUDA, H., KANEKO, Y., "Determination of Large Negative Reactivity by Integral Versions of Various Experimental Methods," *J. Nucl. Sci. & Technol.*, **17**(8), 593, (1980]
- [6.23] LEWINS, J., "The Use of the Generation Time in Reactor Kinetics," *Nucl. Sci. & Eng.*, **7**, 122, (1960)
- [6.24] DIFILIPPO, F.C., "LEU-HTR PROTEUS: Neutron Kinetics and Procedures to Analyze Pulsed Neutron Experiments," PSI Internal Report TM-41-91-27, Oct. 1991.
- [6.25] WILLIAMS, T., "ALPHUBEL - A FORTRAN Code for Use in the Analysis of Pulsed-neutron Source Measurements (Version 1.00)," PSI Internal Report TM-41-91-31, Nov 1991.
- [6.26] GOZANI, T., "The Concept of Reactivity and its Application to Kinetic Measurements," *Nukleonik*, **5**, 55, (1962)
- [6.27] WILLIAMS, T., "Version 2.00 of ALPHUBEL.FOR," PSI Memorandum dated 20.11.91
- [6.28] WILLIAMS, T., "Version 2.01 of ALPHUBEL.FOR," PSI Memorandum dated 18.12.91
- [6.29] WILLIAMS, T., "Further Validation of the ALPHUBEL Suite (Version 2.00) Using Results from Simulated Experiments", PSI Internal Report TM-41-91-39, Dec. 1991.
- [6.30] CARO, M., DIFILIPPO, F. C., "Simulation of the Pulsed Neutron Source Experiment," PSI Internal Report TM-41-91-41, Dec. 1991.
- [6.31] F. C. DIFILIPPO, M. CARO, T. WILLIAMS, "Simulation of Pulsed Neutron Source Reactivity Measurements," *Proc. Joint Int. Conf. on Maths. Methods and Supercomputing in Nucl. Applications*, April 19-23, 1993, Karlsruhe.
- [6.32] MOREIRA, J., LEE, J.C., "Space-Time Analysis of Reactor-Control-Rod Worth Measurements," *Nucl. Sci. & Eng.*, **86**, 91, (1984)
- [6.33] DIFILIPPO, D.C., "LEU-HTR PROTEUS: Theory and Simulations of Reactivity Measurements with the Inverse Kinetics Method," PSI Internal Report TM-41-91-38, Apr 1992

- [6.34] WILLIAMS, T., "IVK - A FORTRAN Code for use in the Analysis of "Inverse-Kinetics" Measurements (version 1.00)," PSI Internal Report TM-41-92-10, May 1992
- [6.35] SCHERER, W., DRÜKE, V., GERWIN, H., PRESSER, W., " Adaptation of the Inverse Kinetic Method to Reactivity Measuremnts in the Thorium High-Temperature Reactor-300," Nucl. Sci. & Eng.,**97**, 96, (1987)
- [6.36] HOGAN, W. S.," Negative Reactivity Measurements," Nucl. Sci. & Eng., **8**, 518, (1960)
- [6.37] KAHTER reference on IVK
- [6.38] WILLIAMS, T., "Planning and Interpretation of Inverse Kinetics Experiments in LEU-HTR Configurations of the PROTEUS Facility" PSI Annual Report, Annexe IV, 1992.
- [6.39] WILLIAMS, T., " HTR-PROTEUS CORE 1: ZEBRA Control Rod S-Curves and Rest Worths," PSI Internal Report TM-41-92-40, Feb. 1993
- [6.40] WILLIAMS, T., " HTR-PROTEUS Core 1A: The Replacement of the ZEBRA Control-Rods by Conventional Control-Rods," PSI Internal Report TM-41-93-25, Aug. 1993.
- [6.41] WILLIAMS, T., "Stable Period Measurements in HTR PROTEUS," PSI Memorandum dated 12 June 1992
- [6.42] Behringers report on the fast channel
- [6.43] LABVIEW Internal PSI Memo
- [6.44] WILLIAMS, T.," Preliminary Investigation of Neutron Noise Measurements on HTR-PROTEUS," PSI Internal Report TM-41-90-30, Aug. 1990
- [6.45] LEBEDEV, G. V., WILLIAMS, T.," Preliminary Investigation of Stochastic Techniques to the Measurement of Absolute Power and Kinetics Parameters in HTR-PROTEUS," PSI Internal Report TM-41-94-18, September 1994.
- [6.46] WALLERBOS, E.J.M.," Investigation of the Application of Noise Techniques to HTR-PROTEUS," PSI Internal Report TM-41-94-24, Jan. 1995
- [6.47] SPRIGGS, G.D.," , Nucl. Sci. & Engng., **113**, 161 (1993)
- [6.48] YASUDA, H., MIYOSHI, R.,"Application of Polarity Correlation Method to Graphite Moderated Reactor," J. Nucl. Sci. Technol., **9**, 544 (1972)
- [6.49] KANEKO. Y.,"Reactor Physics Research Activities Related to the Very High Temperature Reactor in Japan," Nucl. Sci. Eng., **97**, 145 (1987)
- [6.50] AKINO, F. et al.,"Critical experiments on Initial Loading Core of Very high Temperature Reactor Critical Assembly (VHTRC)," Presented at Consultants Meeting at PSI 1989
- [6.51] SHIMAKAWA, S. et al.," Critical Experiments of JMTRC MEU Cores (II)," Proc. Int. Mtg. on Reduced Enrichment for Research and Test Reactors, Petten, the Netherlands, Oct 14-16, 1985.
- [6.52] MISAWA, T. et al.,"Measurement of Prompt Neutron Decay Constant and Large Subcriticality by the Feynmann α Method," Nucl. Sci. Eng., **104**, 53 (1990)
- [6.53] GMÜR, K.,"Techniques of Reaction Rate Measurements on the PROTEUS Reactor", EIR (became PSI) Report No. 529 (1984)

- [6.54] MATHEWS, D., "Foils vs. Particles - Revised," PSI Memorandum dated 24 May 1994
- [6.55] KÖBERL, O., "Untersuchungen zur γ -Selbstabsorption in graphitfolien mit LEU-Partikeln," PSI Memorandum dated 11 April 1994
- [6.56] KÖBERL, O., "Untersuchungen zur γ -Selbstabsorption in graphitfolien mit LEU-Partikeln, Teil II," PSI Memorandum dated 9 Juni 1994
- [6.57] BAARD, J.H., "Nuclear Data Guide to Reactor Neutron Metrology," Kluwer Academic Publishers, 1989
- [6.58] "X-Ray and Gamma-Ray Standards for Detector Calibration," IAEA-TECDOC-619, (1991)
- [6.59] KÖBERL, O., " γ -Selbstabsorptionskorrekturen für LEU-AVR Brennstoffkugeln und Partikel mit homogener Quellverteilung," PSI Internal Report TM-41-94-20, (1994)
- [6.60] MATHEWS, D., "Sensitivity to Graphite absorption etc.," PSI Memorandum dated 14.6.91 (also Private Communication with T. Williams dated 29.5.92)
- [6.61] DIFILIPPO, F.C., " PNS Measurements of Effective Graphite Absorption," PSI Internal report TM-41-91-32, Nov 1991
- [6.62] VALENTE, F.A., " A Manual of Experiments in Reactor Physics," pp. 94-124, The Macmillan Co., New York, 1963